EUR 4468 e

FORCED CONVECTION BURNOUT
AND HYDRODYNAMIC INSTABILITY EXPERIMENTS
FOR WATER AT HIGH PRESSURE

Part VI: Burnout heat flux measurements on 9 rod bundles with longitudinally and transversally uniform heat generation

by

A. CAMPANILE, G. GALIMI, M. GOFFI and G. PASSAVANTI
(SORIN, Centro Ricerche Nucleari, Saluggia, Italy)

1970

EUR 4468 e

FORCED CONVECTION BURNOUT AND HYDRODYNAMIC INSTA-
BILITY EXPERIMENTS FOR WATER AT HIGH PRESSURE
Part VI: Burnout heat flux measurements on 9 rod bundles with longitu-
   dinally and transversally uniform heat generation
by A. CAMPANILE, G. GALIMI, M. GOFFI and G. PASSAVANTI
(SORIN, Centro Ricerche Nucleari, Saluggia - Italy)

European Atomic Energy Community - EURATOM
FIAT S.p.A., Sezione Energia Nucleare - Torino
Società ANSALDO S.p.A. - Genova
Contract No. 008-61-12 PNII
Luxembourg, May 1970 - 46 Pages - 25 Figures - FB 70.

   This report presents 235 burnout points obtained on a 3 × 3 square array
of 10.2 mm O.D. Inconel tubes generating the same power with a uniform
power distribution over a 1183 mm length.

The rod bundle was tested in two square channels having different flow area.

Burnout was found to occur at locations in the lattice depending on the spacing between external rods and unheated surfaces as well as on physical test conditions.

Whenever possible, measurements of the exit water temperatures and pressure drops were also taken.

The rod bundle was tested in two square channels having different flow area.

Burnout was found to occur at locations in the lattice depending on the spacing between external rods and unheated surfaces as well as on physical test conditions.

Whenever possible, measurements of the exit water temperatures and pressure drops were also taken.

The rod bundle was tested in two square channels having different flow area.

Burnout was found to occur at locations in the lattice depending on the spacing between external rods and unheated surfaces as well as on physical test conditions.

Whenever possible, measurements of the exit water temperatures and pressure drops were also taken.

EUR 4468 e

FORCED CONVECTION BURNOUT
AND HYDRODYNAMIC INSTABILITY EXPERIMENTS
FOR WATER AT HIGH PRESSURE

Part VI: Burnout heat flux measurements on
9 rod bundles with longitudinally and
transversally uniform heat generation

by

A. CAMPANILE, G. GALIMI, M. GOFFI and G. PASSAVANTI
(SORIN, Centro Ricerche Nucleari, Saluggia, Italy)

1970

ABSTRACT

This report presents 235 burnout points obtained on a 3 × 3 square array of 10.2 mm O.D. Inconel tubes generating the same power with a uniform power distribution over a 1183 mm length.

The rod bundle was tested in two square channels having different flow area.

Burnout was found to occur at locations in the lattice depending on the spacing between external rods and unheated surfaces as well as on physical test conditions.

Whenever possible, measurements of the exit water temperatures and pressure drops were also taken.

KEYWORDS

Index

Reports on <u>FORCED CONVECTION BURNOUT AND HYDRODYNAMIC INSTABILITY</u>
<u>EXPERIMENTS FOR WATER AT HIGH PRESSURE</u> already published:

EUR 2490 e - Part I: Presentation of Data for Round Tubes with
(Full-size)   Uniform and Non-uniform Power Distribution (1965).

EUR 2963 e - Part II: Presentation of Data for Water Flowing Upward
(Full-size)   Along a Uniformly Heated Rod in a Square
                    Unheated Duct (1966).

EUR 3113 e - Part III: Comparison Between Experimental Burnout Data
(Full-size)   and Theoretical Prediction for Uniform and
                    Non-uniform Heat Flux Distribution (1966).

EUR 3881 e - Part IV: Burnout Experiments in a Double Channel Test
(Full-size)   Section with Transversely Varying Heat
                    Generation (1968).

EUR 4070 e - Part V: Analysis of Heating and Burnout Experiments in
(Full-size)   a Double Channel Test Section with Transversely
                    Varying Heat Generation (1968).

FORCED CONVECTION BURNOUT AND HYDRODYNAMIC INSTABILITY EXPERIMENTS FOR WATER AT HIGH PRESSURE *)

1. Introduction

To improve the understanding of the basic mechanisms of
the boiling crisis is a target much longed for in water
reactor engineering because of the advances in economic in
centives and reactor safety that would result from a refin
ed ability of assessing burnout power limits.

Yet, the known picture of the mechanisms is far from be
ing complete and there are still many features relevant to
the problem that must be explained, although continued pro
gress is being made in gaining deeper insight into the boil
ing phenomena.

The status of knowledge of the boiling crisis being still
uncertain, the approach to meet the need of providing reac-
tor designers with working formulas of reasonable length and
complexity, has been to attempt comprehensive correlations
of numerous burn-out heat flux experimental data taken on
test sections of relatively simple geometry.

This work enabled to prescribe purely empirical equations
which yield sufficient accuracy for technical purposes, ir-
respective of special effects and physical functional depen
dencies among the variables involved.

The empirical character of the correlations so far develop
ed from data taken using channels of simple geometry, makes
their straightforward application to geometries of complex
cross sections difficult and questionable.

The peculiar features of a multi-rod cluster assembly,
which presents geometry characteristics identical with those
prevailing in water cooled reactor core, claim that at least

two basic problems be solved prior to applying conclusions and correlations drawn from single heater tests to rod bun dle assemblies:

- to find a method of combining, on a sound theoretical basis, special effects, singularly identified and examin ed in experiments performed on channels of simple cross sections, when they are, as in the case of a rod cluster, present all together presumably modifying the action each would exert in the absence of the others.

- To take properly into account the degree of interconnec- tion of coolant channels in an open rod matrix starting from the most suitable subdivision of the entire flow conduit in an array of subchannels. This analysis should ultimately lead to the evaluation of local flow rate and enthalpy values.

These problems have been so far tackled by developing more or less simple theoretical flow models that account for the turbulent exchange processes taking place between adjacent subchannels in a multi-rod fuel bundle. Such an analysis starts from the subdivision of the total flow passage into a convenient number of smaller sub-passages. This approach is regarded as an alternative to full scale simulation experi- ments, being not readily obvious that such very expensive and time consuming experiments would indeed simulate the actual core conditions or, in any case, would produce information of value comparable to the cost and efforts required for these experiments to be carried out.

The plausibility of the assumptions underlying a theo-
retical flow model must obviously be checked by comparing
the predictions of the model against the results of relati
vely simpler simulation experiments performed in a wide
range of conditions. The disposable coefficients introduc
ed in the model are eventually adjusted by choosing their
values so as to make predictions match experimental data.

This is the context in which the present experimental
investigation on the boiling burnout in a rod bundle test
section was undertaken.

The experiments were conducted on a square pitch array
of 9 rods electrically heated and cooled by water at high
pressure flowing axially.

The study aimed at the determination of burnout heat
fluxes in uniformely heated bundles as well as in bundles
characterized by radial heat flux distributions other than
uniform. It was also anticipated to perform experiments on
rod clusters having non uniform axial flux shape.

In addition, it was decided to investigate "unique posi-
tions" in the matrix, such as obstructed subchannels, corner
and side cells, guide tubes, etc., where burn-out might show
traces of peculiar effects.

The experiments here referred to concerns burnout in uni-
formly heated bundles only.

The subject of typical influences related to unsymmetrical
conditions either in the heat generation or in the channel
geometry, will be covered in a separate report.

This study was conducted by SORIN as part of a R & D. pro
gram supporting the design of a pressurized water reactor for
ship propulsion developed by FIAT in the frame of a contract

with EURATOM, CNEN and ANSALDO.

A large part of the experiments here referred to were con ducted at the Joint Nuclear Research Center in Ispra by cour tesy of the EURATOM which allowed us to take advantage of the fruitful cooperation and assistance of the Heat Transfer Laboratory Staff and to use their high pressure experimental loop.

2. Experimental facilities

2.1. Test loops

Two high pressure loops were used to perform the cluster burnout experiments here reported, namely the 650 kW SORIN loop of Saluggia Research Center and the 2400 kW EURATOM loop of ISPRA Joint Nuclear Research Center .

The test loops and the operating procedures were essen- tially the same as those described in details in Ref. /1/ and /2/.

As for the SORIN loop the major modification concerned the by-pass line being, in the present layout, provided only to the purpose of condensing the steam contained in the fluid at the exit of the heated channel by mixing it with suboooled water. It was no longer supposed to impose a constant pressure drop across the test section.

2.2. Test section

The test section, as shown in Fig. 1, consisted basically of a vertical pressure vessel with a square flow channel housing a 9 rod cluster arranged on a 3 x 3 square pitch pattern.

The high heat flux zone of the heaters was made of thin-wall Inconel X - 750 tubing, 10.2 mm O.D. placed on 13.4 mm centers, with a uniformly heated length of 1183 mm.

The walls of the nine rods were 0.38 mm thick. Beyond either end of this zone, the heat flux was sharply reduced. In fact, each Inconel heater tube was welded at both ends to stainless steel connection rods of the same O.D. as the tube, the upper connection being a 500 mm long solid rod whereas the lower one was made of a 500 mm tubing 2 mm thick.

The nine rods were connected in parallel across the power supply bus-bars. At the lower end the connection was made by means of a common terminal plate acting as a stationary tube sheet of a removable - bundle type shell and tube heat exchanger. Nine holes were drilled in this plate on the same square pattern as that of the bundle; the tubes were inserted inside the holes and welded to the tube sheet.

This was clamped between the bottom flange of the pressure vessel and the flange of the gas pressurization cover and electrically insulated from them.

The latter arrangement allowed to balance the external pressure by pressurizing the rods internally through the gas pressurization cover, thus preventing the thin-wall tubes collapse at burnout conditions.

The electrical parallel connection at the top end was accomplished by individually coupling each rod to a common plate through a flexible copper terminal having tapered mechanical joints at both ends. Additional flexibility to the system was offered by the stranded copper cable connect ing this top plate to the ground potenzial bus bar attached to the side closure flange of the containment vessel. Corrosion of the copper electrode was avoided by inserting it in a corrugated thin wall stainless steel tube.

To prevent bowing of the rods, the bundle was put in tension as a whole by a large Inconel spring, intermediate individual small springs being also provided to assure ade guate allowance for differences in thermal expansion of each rod at burnout.

The spacing between the rods was maintained by using five grids equally spaced 252 mm apart along the heated portion of the bundle. The highest grid was installed about 150 mm upstream of the burnout position.

The grids consisted essentially of a thin square can, having the same internal side as that of the flow channel, and of 16 ferrules 15 mm high.

The side and corner ferrules were respectively made of halves and quarters of thin stainless steel tubing brazed to the can, whereas the four central ones consisted simply of removable short cylindrical pieces of the same tube.

Details of the grids are shown in Fig. 2.

Two additional grids were located respectively upstream and downstream the heated portion of the bundle.

At the inlet, a distance for the grid of about 358 mm from the lower end of the active zone was considered ade-

quate for flow re-establishment.

The square flow channel was made of four side plates whose relative position could be changed within certain limits. This arrangement allowed to prepare flow channels of different cross-sectional area using always the same plates.

For each selected relative position, the four plates were fastened together by screwed coupling. The mating faces of the plates at each corner were finely machined and the facing was of the raised face and groove type with a teflon cord as gasket.

The necessary electrical insulation between the Inconel heater tubes and the flow housing, was obtained by coating each surface of the four side plates facing the bundle with special aluminum - oxide ceramic tiles machined to strict tolerances and with lapped surface finishing.

Water entered the test section at the bottom through a flanged side nozzle, flowing upward parallel to the bundle and leaving the channel axially through the top throat of the pressure vessel directly flanged to the loop.

A suitable seal between the pressure vessel and the flow channel prevented water by-passing the heater bundle.

An exploded view of the test section is shown in Fig. 3.

2.3. Measurements and control

Throughout the experiments the following quantities were measured:

- Electrical power generated in the rod active length

- Coolant flow

- Coolant inlet temperature at two points of the flow area

- Coolant outlet temperatures at six points of the flow area located as shown in Fig. 4

- Static pressure at the outlet end of the rod active length

- Pressure drop over the channel active length

The inlet and exit water temperatures were measured by sheath type stainless steel jacketed thermocouples insert ed from the outside of the pressure vessel to the select- ed positions of the rod bundle flow passage by means of suitably designed pressure tight and electrically insulat ed threaded plugs.

Pressure tapping were brought out the test section through the annular gap between the flow channel and the containment vessel using flexible pipes.

Burnout detection was accomplished by means of sheath type thermocouples inserted in the heater tubes with the hot junction looking out on the interior wall of the tube very near the termination of heating were burnout was most likely to occur.

Each thermocouple was stiffened by a metallic rod and inserted in a pyrex tubing. This installation provided electrical insulation of the thermocouples from the Inconel heaters and assured adequate allowance for a quick detec-

tion of wall temperature excursions.

The nine pyrex tubes of the burnout detection device were inserted into the rods through the holes of lower bundle tube shee↑ and the thermocouples leads were brought out the test section through the gas pressurization cover.

In some experiments each heater was equipped with two B.O. thermocouples, the second one being positioned at the location of the ferrules of the grid closest to the outlet.

3. Experimental program

The data here referred to were obtained on two square channels of different flow area both housing an identical heater rod bundle.

Capital letters A and B will be used throughout the paper to designate the channel having shorter and larger side respectively.

The latter is, obviously, characterized by a greater distance between the unheated containment walls and the outer heated rods.

Fig. 5 shows the cross sections of the two tested configurations and their most relevant dimensional data.

The criterion adopted in designing channel B was to attain an approximatively equal distribution of the total flow among the coolant cells of the different rods in the cluster.

By introducing the term "coolant cell of a rod", it is not intended to make here any statement about the portion of cool ant actually associated to one rod of a bundle in the process

of heat transfer; it is rather proposed a schematization in subdividing the total flow area in a suitable manner among the different rods. Such a schematization is indicat ed in Fig. 5.

The larger coolant area associated to the side rods, and even more to the corner rods, was supposed to compensate the unfavourable flow conditions of these subchannels resulting from their more extended wetted perimeter.

Obviously this compensation doesn't hold for all the three characteristic cells at the same time, least of all it is maintained while varying the coolant conditions during an experiment.

Therefore it is worth to stress again the fact that the B configuration aimed only at the achievement of a total flow distribution among the different subchannels more uniform than in channel A. With this arrangement, in fact, un like channel A in which burnout did always occur on corner rods only, the burnout inception was observed on any one of the rods set at the three characteristic positions in the bundle, i.e. central, side and corner, burnout being detect ed at only one or more than one of these locations according to the experimental conditions.

Table I reports the most relevant data concerning the tested channels.

4. Experimental results

4.1. Test parameters ranges

The experiments were done under different physical con ditions according to the ranges listed below:

Pressure: from 84 to 158 Kg/cm^2

Mass flow rate: from 50 to 300 gr/cm^2 sec

Inlet temperature: from 194 to 322°C

The range of dependent variables were experimentally found as follows:

Burnout heat flux: from 87 to 286 $watt/cm^2$

Exit quality: from -34% to +53%.

4.2. Tabulation and graphical representation

The burnout and pressure drop results are tabulated in Tables II through XI. The data available for channel A are presented in Tables II through V followed by the chan nel B data in Tables VI through XI. In each group a sepa rate table is used for each pressure; within each table data are listed in order of increasing and decreasing ma- gnitude of the mass flow rate and inlet temperature respec tively.

The power values which have been tabulated·represent
the heat generated in the active length of 9 rod bundle
at burnout.

For each run, the occurrence of the burn-out in one or
more of the typical cells of the lattice has been report-
ed.

The values of the water exit temperature listed in the
tables have been obtained as the arithmetic mean of values
measured in symmetric positions in the flow area.

The locations of the respective temperature probes are
shown in Fig. 4.

Reported values of pressure drop refer to measurement
taken, at burn-out inception, across the channel active
length. These values account also for the elevation pres
sure drop.

Fig. 6 through 25 show the values of the burnout
rod power plotted against their inlet temperatures. These
values were calculated as 1/9 of the power generated on the
active length of the bundle.

In order to allow location of the various rods on which
burnout was detected, the plots make use of different sym-
bols, whose interpretation key is reported in Table XII.

It can be seen that a single symbol have been used for
the tests made on channel A, the burnout being always detect
ed in this case, as previously remarked, on corner rods only.

Conversely, in channel B, burnout did not occur always at
a unique position in the lattice. The experiments did rather
show a definite link between the burnout location and the
coolant conditions (pressure, inlet temperature and mass flow
rate).

5. Some remarks on the experimental results

The trend of the experimental burnout data, as shown in the plots herein presented, suggests the following remarks:

- In the channel A, the exclusive occurring of the burnout throughout the tests on the rods located in corner position, would indicate that in this channel, the cooling and flow conditions in the corner cells, which offer the same flow area to the passage of the coolant as the other ones in the lattice, are always adversely affected.
  This might well be related to the proximity of unheated surfaces to the corner rods as well as to the more extend ed wetted perimeter of these cells.

- Conversely, in the channel B, a definite link was observed between the main coolant parameters, such as pressure, mass flow rate and inlet temperature, and the positions in the lattice in which the burnout was first revealed.

Throughout the experiments conducted at the highest of tested pressure values, the burnout inception was always de tected on the central rod only.

At lower values of this parameter, the behaviour was entirely different as far as burnout location in the lattice was concerned.

The burnout was generally detected in one or more of the three typical subchannel simultaneously, the specific location for each case being strictly related to the experimental conditions.

In general, for a given mass flow rate, the burnout was
never detected on the central rod in the range of the high-
est inlet temperature values, whereas in the lowest inlet
temperature range, the corner rods were never involved in
the thermal crisis process. To the intermediate values of
the inlet temperature corresponds a transition region; here
the burnout did occur at the three typical positions simul-
taneously. To summarize, at low pressure, and markedly at
low mass flow rate, the trend was as follows:

| CENTRAL ROD | CENTRAL ROD SIDE ROD | CENTRAL ROD SIDE ROD CORNER ROD | SIDE ROD CORNER ROD | CORNER ROD |

———— Increasing Inlet Temperature ————⟶
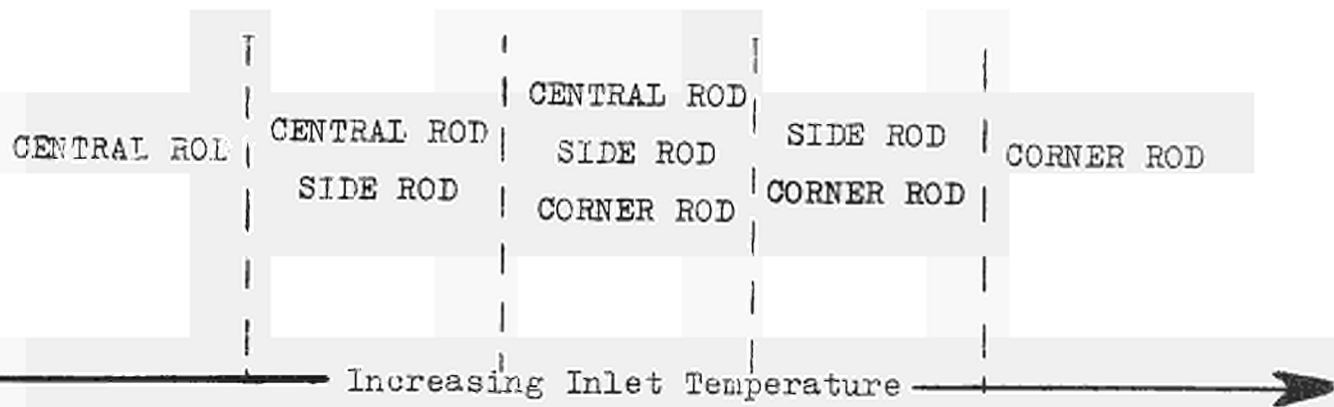
With increasing the mass flow rate, the aforesaid transi-
tion region, appeared to be shifted toward higher values of
the inlet temperature, that is to say, the burnout inception

on the central rod was detected in a wider range of inlet temperature. Thus, from burnout location stand point, an increase of the mass flow rate could be seen as equivalent to an increase of the pressure.

One might infer by analyzing the experimental results, a close connection between positions in the lattice where burnout is most likely to occur, and the volumetric steam flow rate in the channel.

The observed trend of the points, would indicate that beyond certain values of the steam quality, the adverse in fluence of the unheated surfaces delimiting the corner cells, starts prevailing over the favourable flow conditions of these cells wich, in the channel B, have a larger associated flow area as compared to the other ones.

So far we have examined the data referring to the two extreme values of the pressure tested in our experiments.

One could anticipate that, for given values of the mass flow rate and inlet temperature, the burnout will start con cerning potions other than the central one as the pressure decreases from the higher value to an intermediate transi- tion one.

To substantiate this anticipation, a limited number of experiments was conducted at intermediate values of the pres sure, which led to an experimental confirmation of the exi- stence of such a transition pressure.

Acknowledgements

References

/1/ F. Biancone, A. Campanile, G. Galimi, M. Goffi, "Forced convection burnout and hydrodynamic instability experiments for water at high pressure. Part I: Presentation of data for round tubes with uniform and non-uniform power distribution", Report EUR 2490.e, 1965

/2/ H. Herkenrath, P. Mörk-Mörkenstein, "2,4 MW Druck-und Siedewasserkreislauf zur Untersuchung des Wärmeübergangs", EUR 3605 d, 1967.

TABLE I

Relevant data of the channels A and B

		A			B		
		Central cell	Lateral cell	Corner cell	Central cell	Lateral cell	Corner cell
Equivalent diameter	mm	12.2	8.61	6.65	12.2	9.86	8.37
Equivalent diameter based on the heated perimeter	mm	12.2	12.2	12.2	12.2	14	15.9
Rod diameter	mm	10.2					
Lattice pitch	mm	13.4					
Heated length	mm	1183					
Total number of grids		7					
Number of grids in the heated length		5					
Heat flux distribution		uniform					

Burnout experiments data on Channel A

TABLE II

Nominal pressure: 84 ata

Run	Pressure ata	Flow l/h	Mass flow rate gr/cm2 sec.	Inlet °C Subcooling	Inlet °C Temperature	Exit temperature °C			Power Kw.	Average heat flux watt / cm2	Exit quality %	Bournout Rods position in the lattice			Pressure Drop gr/cm2
						a	b	c				Central	Side	Corner	
74 (25-6-68)	86	2100	52,11	37,5	261,2	295,5	295,5	295,5	414,7	121,5	49,95			*	119
10 (24-6-68)	88	2020	50,9	46,1	253,5	294,9	294,9	294,9	419,4	122,9	49,35			*	109
27 (25-6-68)	87	1950	50,91	66	233,5	296,0	296,0	296,0	415,7	121,8	42,08			*	
15 (25-6-68)	88	1920	52,03	91,3	209,0	297,2	297,2	297,2	482,1	141,3	42,86			*	118
169 (25-6-68)	86,5	3980	93,65	15,1	284,0	295,5	295,5	295,5	506,1	148,3	37,59			*	222
109 (25-6-68)	89	3860	91,79	20,9	280,2	297,2	297,2	297,2	544,6	159,6	40,04			*	211
46 (25-6-68)	86	3770	92,49	32,2	266,5	296,2	296,2	296,2	551,4	161,6	35,79			*	
190 (25-6-68)	86	6830	157,59	7,5	291,2	296,7	296,7	296,7	574,8	168,5	26,29			*	380
137 (25-6-68)	86	6600	154,79	13,5	285,2	295,0	295,0	295,0	595,1	174,4	25,59			*	360

Burnout experiments data on Channel A

TABLE III

Nominal Pressure: 115 ata

Run	Pressure ata	Flow l/h	Mass flow rate gr/cm²sec.	Inlet °C Subcooling	Inlet °C temperature	Exit temperature °C			Power Kw.	Average heat flux watt/cm2	Exit quality %	Burnout Rods Position in the lattice			Pressure Drop gr/cm2
						a	b	c				Central	Side	Corner	
68 (20-6-68)	118	2220	51,07	27,0	294,9	318,0	318,0	318,0	343,7	100,7	49,45			*	104
39 (20-6-68)	117,5	2110	50,99	45,8	275,7	319,0	319,0	319,0	371,1	108,8	46,35			*	
34 (19-6-68)	116,5	2050	51,96	68,4	252,5	317,1	317,7	317,7	408,7	119,8	42,56			*	106
9 (19-6-68)	114	1960	51,49	87,8	231,5	314,3	314,7	314,7	439,8	128,9	41,03			*	104
87 (20-6-68)	114	4180	96,4	25,6	293,7	316,7	316,7	316,7	443,5	130,0	29,85			*	171
35 (20-6-68)	111,5	4020	97,64	44,6	273,0	315,5	315,3	315,3	487,7	142,9	25,3			*	168
16 (20-6-68)	114,5	3770	93,08	53,9	265,7	317,0	317,0	317,0	517,3	151,6	26,87			*	
42 (19-6-68)	116,5	3750	93,52	59,9	261,0	318,5	319,0	319,0	509,3	149,3	23,56			*	
50 (19-6-68)	115	3750	93,79	60,4	259,5	316,4	316,5	316,5	511,6	149,9	23,36			*	155
27 (19-6-68)	113,5	3610	92,93	75,2	243,7	314,2	314,7	314,7	565,3	184,1	23,3			*	129
76 (20-6-68)	113	6890	158,86	24,9	293,7	315,8	315,8	315,8	527,7	154,6	18,43			*	273
57 (20-6-68)	113,5	6610	156,96	36,2	282,7	316,5	316,5	316,5	592,2	173,6	17,72			*	267
29 (20-6-68)	121	6300	153,63	51,8	272,0	320,2	320,2	320,2	614,1	180,0	13,45			*	240

Burnout experiments data on Channel A

TABLE IV

Nominal pressure: 132 ata

Run	Pressure ata	Flow l/h	Mass flow rate gr/cm²sec.	Inlet °C Subcooling	Inlet °C temperature	Exit temperature °C a	b	c	Power Kw.	Average heat flux Watt/cm²	Exit quality%	Burnout Rods Position in the lattice Central	Side	Corner	Pressure Drop gr/cm²
58 (7-6-68)	136,5	2140	50,38	44,9	288,2	329,8	329,8	329,8	334,4	98,0	43,63			*	101
45 (7-6-68)	133	2060	50,51	60,6	270,5	327,5	327,5	327,5	362,7	106,3	41,48			*	101
20 (7-6-68)	135,5	2060	51,91	75,5	257,0	329	329	329	385,6	113,0	37,74			*	107
9 (7-6-68)	133,5	2020	52,46	91,3	240,0	327	327	327	404,2	118,5	33,61			*	105
112 (7-6-68)	138	3970	89,25	29,5	304,5	331	331	331	389,7	114,2	28,0			*	145
56 (6-6-68)	137	4090	94,55	38,4	295,0	329,6	329,8	329,9	408,5	119,7	23,0			*	128
67 (7-6-68)	135,5	4040	95,72	47,0	285,5	329,5	329,5	329,5	449,1	131,6	22,61			*	145
19 (6-6-68)	133,5	3780	90,79	51,5	279,8	329,1	329,3	329	444,4	130,2	22,5			*	
33 (6-6-68)	136	3720	94,81	81,8	251	329,3	329,3	329,3	507,1	165,0	13,78			*	128
95 (7-6-68)	136,5	7180	161,09	28,1	305,0	330,25	330,25	330,25	495,1	145,1	15,28			*	238
80 (7-6-68)	138,5	6750	156,1	39,2	295,0	331,5	331,5	331,5	531,1	155,7	13,12			*	216
41 (7-6-68)	133,5	6260	154,31	63,3	268,0	328	328	326,5	606,1	177,6	7,49			*	200
125 (7-6-68)	138,5	10230	226,46	24,7	309,5	331	331	331	556,6	163,1	10,65			*	314
87 (7-6-68)	136	9760	226,38	39,1	293,7	329	329	329	625,4	183,3	6,64			*	307

Burnout experiments data on Channel A

<u>TABLE V</u>

Nominal pressure: 144 ata

Run	Pressure ata	Flow l/h	Mass flow rate gr/cm²sec.	Inlet °C Subcooling	Inlet °C temperature	Exit temperature °C			Power Kw.	Average heat flux watt/cm²	Exit quality%	Burnout Rods Position in the lattice			Pressure Drop gr/cm²
						a	b	c				Central	Side	Corner	
60 (18-6-68)	142,5	2280	50,82	28,8	307,7	333,5	333,5	333,5	297,9	87,3	44,61			*	96
134 (7 - 6-68)	144,5	2275	51,25	33,1	301,5	334,7	334,7	334,7	300,3	88,0	42,64			*	98
62 (14-6-68)	145,5	2300	52,03	34,8	303,3	335,8	335,9	335,8	296,6	86,9	40,18			*	40
29 (18-6-68)	145	2230	51,14	39,1	298,7	334,7	334,7	334,7	307,5	90,1	41,2			*	96
38 (18-6-68)	145,5	1970	46,42	49,4	288,7	335,1	335,1	335,1	325,1	95,3	46,83			*	96
49 (14-6-68)	143,5	2180	51,78	51,8	285,2	334,7	334,7	334,7	331,6	97,2	38,88			*	43
60 (12-6-68)	147,5	2070	50,89	68,7	270,5	336,2	336,2	336,2	346,5	101,6	35,62			*	96
30 (12-6-68)	143,5	2000	50,55	81,0	256,0	334,7	334,7	334,7	370,3	108,5	35,06			*	98
67 (14-6-68)	145,5	4250	94,24	28,3	309,8	337,5	337,5	337,5	376,1	110,2	25,15			*	142
72 (18-6-68)	145,5	4200	93,73	30,4	307,7	336,0	336,0	336,0	380,1	111,4	24,72			*	142
108 (12-6-68)	147,5	4130	93,67	36,5	302,7	336,2	336,2	336,2	404,3	118,5	24,41			*	138
54 (18-6-68)	145	4050	93,01	39,6	298,2	334,9	335,1	334,9	401,5	117,7	22,65			*	97
25 (14-6-68)	142,5	4030	94,46	46,0	290,5	333,5	333,5	333,5	423,4	124,1	21,18			*	96
52 (12-6-68)	145,5	3830	94,12	67,6	270,5	335,8	335,3	334,7	472,4	138,5	16,56			*	138
18 (18-6-68)	145,5	3830	94,12	67,6	270,5	335,75	335,6	334,5	483,9	141,8	17,88			*	138
15 (12-6-68)	143	3670	93,59	85,5	251,2	334,6	334,7	334,0	498,9	146,2	11,72			*	134
81 (14-6-68)	146,5	7160	154,25	21,0	317,7	336,5	336,5	336,5	436,3	127,9	16,8			*	211
75 (12-6-68)	146	6750	157,27	45,4	293,0	336,5	336,5	336,1	512,6	150,2	8,31			*	196
38 (12-6-68)	147,5	6220	154,0	72,2	267,0	335,7	334	329	559,9	164,1	−0,8			*	174
95 (14-6-68)	144	10330	224,28	22,0	315,3	334,1	333,5	334,2	521,2	152,7	10,72			*	325
36 (14-6-68)	144,5	9660	223,82	42,7	294,9	334,2	334,8	333,8	602,6	176,6	3,64			*	269

- 21 -

Burnout experiments data on channel B   <u>TABLE VI</u>

Nominal pressure: 84 ata

Run	Pressure ata	Flow 1/h	Mass Flow rate gr/cm2 sec.	Inlet °C Subcooling	Inlet °C Temperature	Exit temperature °C			Power Kw.	Average heat flux watt/cm2	Exit quality %	Burnout Rods Position in the lattice			Pressure drop gr/cm2
						a	b	c				Central	Side	Corner	
32 (15-7-69)	84,2	2535	48,9	4,4	292,7	294,8	296,7	297,0	394,8	115,8	50,8			*	-
27 (15-7-69)	83,0	2450	48,3	12,4	283,7	296,0	296,0	296,5	410,9	120,3	50,5			*	-
112(7-2-68)	82,0	2540	50,4	15,6	279,7	294,0	295,8	-	453,4	132,9	53,4		*	*	100
84 (1-3-68)	85,5	2560	50,9	19,1	279,1	294,0	-	-	457,9	134,2	52,8		*	*	123
80 (8-1-68)	82,8	2500	50,6	23,8	271,5	296,0	298,0	-	462,9	135,7	51,5		*	*	104
8 (8-2-68)	84,0	2420	49,0	25,5	271,5	294,2	294,4	-	449,5	131,7	51,4		*	*	98
27 (23-5-69)	86,0	2462	49,9	27,2	271,5	289,2	298,4	299,2	437,5	128,5	47,6		*	*	-
97 (7-2-68)	84,5	2460	50,0	27,9	269,5	295,1	296,7	-	456,9	133,9	50,3		*	*	109
40 (4-3-68)	83,5	2400	49,9	37,9	258,7	-	-	-	481,4	141,1	50,0		*	*	109
23 (4-3-68)	85,5	2360	49,6	44,8	253,5	-	-	-	484,0	141,9	48,8		*		103
32 (23-5-69)	84,7	2370	49,8	44,8	252,8	288,0	297,3	297,6	475,0	139,3	46,4		*	*	-
84 (7-2-68)	80,5	2360	49,8	43,0	251,1	292,0	293,0	-	499,5	146,4	50,4		*	*	112
122(1-3-68)	81,0	2420	51,6	49,1	245,4	-	-	-	525,2	153,9	49,4	*	*	*	113
9 (4-3-68)	87,0	2320	49,8	56,9	242,6	-	-	-	515,3	151,0	48,9	*	*	*	107
67 (8-2-68)	84,0	2340	50,3	56,0	241,0	292,5	294,7	-	516,2	151,3	48,1	*	*	*	108
48 (4-3-68)	88,5	2250	48,9	66,2	234,5	-	-	-	533,2	156,3	49,7	*	*		102
37 (23-5-69)	83,5	2330	50,6	64,1	232,5	287,6	296,3	296,7	510,7	149,7	43,5		*	*	-
4 (15-7-69)	85,2	2180	48,0	74,5	223,5	287,0	295,5	297,3	511,2	149,8	44,1		*	*	-
54 (4-3-68)	86,5	2290	51,1	71,2	217,9	-	-	-	563,1	165,0	45,3	*	*	*	102
9 (15-7-69)	84,6	2165	48,3	83,8	213,7	290,0	295,0	297,6	538,8	157,9	44,3	*	*		-
15 (15-7-69)	84,9	2145	48,6	95,0	202,7	290,0	294,7	297,7	557,1	163,3	42,9	*			-
21 (15-7-69)	85,3	2125	48,7	103,9	194,2	291,0	296,7	297,7	568,5	166,6	41,6	*	*		-
66 (4-3-68)	83,0	2200	51,1	108,2	188,0	-	-	-	608,7	178,4	42,3	*	*		108
42 (17-7-69)	85,7	4370	84,8	7,9	290,5	-	291,7	-	558,8	163,8	40,0			*	-
109(1-3-68)	90,5	4780	93,1	14,8	287,5	-	-	-	565,1	165,6	35,5		*	*	199
57 (8-1-68)	82,5	4820	94,1	10,0	285,7	292,5	294,5	-	584,2	171,2	37,1		*	*	224

Follows TABLE VI — Burnout experiments data on channel B — Nominal pressure: 84 ata

Run	Pressure ata	Flow 1/h	Mass Flow rate gr/cm² sec.	Inlet °C Subcooling	Inlet °C Temperature	Exit temperature °C			Power Kw.	Average heat flux watt/cm²	Exit quality %	Burnout Rods Position in the lattice			Pressure drop gr/cm²
						a	b	c				Central	Side	Corner	
58 (22-5-69)	83,7	4730	93,0	12,0	284,7	286,2	295,5	296,1	564,5	165,5	34,8			*	-
48 (22-5-69)	84,8	4723	93,1	13,9	283,8	288,2	297,6	298,0	574,0	168,3	35,0			*	-
31 (8-2-68)	82,0	4680	92,7	14,9	280,4	-	296,0	-	596,5	174,8	36,7		*	*	195
45 (22-5-69)	83,5	4688	93,3	16,6	280,0	287,1	296,7	297,1	582,0	170,7	34,3			*	-
82 (4-3-68)	83,5	4680	93,0	21,4	279,2	-	-	-	612,8	179,6	37,1		*	*	-
94 (1-3-68)	82,5	4600	92,1	20,1	275,7	-	-	-	610,7	179,0	36,2		*	*	212
54 (22-5-69)	83,7	4439	90,2	26,8	270,0	287,5	296,6	296,8	618,0	181,2	34,8			*	-
3 (23-5-69)	84,4	4480	92,4	34,9	262,5	288,2	297,1	297,5	622,0	182,3	31,3		*		-
9 (23-5-69)	84,3	4474	92,5	36,0	261,2	288,2	297,0	297,7	637,5	186,9	31,9		*	*	-
15 (23-5-69)	87,2	4365	92,4	50,9	248,8	291,0	299,2	299,8	664,5	194,9	29,2	*	*	*	-
23 (23-5-69)	87,4	4317	92,4	57,8	242,0	292,0	300,0	300,5	692,7	203,1	28,9	*	*		-
28 (17-7-69)	83,2	4270	91,7	56,4	240,0	288,2	-	-	678,3	198,8	28,4	*			-
4 (17-7-69)	84,7	4120	89,8	67,1	230,5	288,8	-	297,0	703,4	206,2	27,9	*			-
9 (17-7-69)	85,1	4080	90,2	77,2	220,7	289,3	-	297,7	707,1	207,2	24,7	*			-
35 (17-7-69)	85,7	4080	90,3	77,9	220,5	-	298,7	-	722,0	211,6	25,6	*			-
15 (17-7-69)	84,5	4040	90,4	85,2	212,2	287,6	-	298,7	721,4	211,4	23,1	*			-
20 (17-7-69)	84,5	3980	90,4	96,4	201,0	284,5	297,2	-	749,5	219,7	21,6	*			-
49 (29-7-69)	85,5	7950	157,0	15,3	283,0	294,4	298,7	300,0	707,0	207,2	23,6	*			-
43 (29-7-69)	83,7	7850	156,6	18,0	278,7	293,5	297,5	299,0	721,0	211,3	23,1	*			-
37 (29-7-69)	84	7665	155,9	27,4	269,6	292,4	297,5	299,0	752,9	220,7	21,3	*			-
34 (29-7-69)	84	7780	161,6	38,0	259,0	291,9	297,7	299,0	800,0	234,5	18,5	*			-
26 (29-7-69)	84,5	7520	158,5	46,4	251,0	292,2	298,2	299,7	820,5	240,5	17,2	*			-
19 (29-7-69)	86	7310	156,3	56,2	242,5	289,3	299,0	300,5	836,0	245,0	15,1	*			-
8 (29-7-69)	83	7110	154,3	62,7	233,5	286,8	297,2	298,5	871,0	255,4	14,9	*			-
13 (22-7-69)	84,5	6680	145,4	65,9	231,5	286,3	297,2	298,5	878,0	257,3	16,4	*			-
55 (29-7-69)	85	7080	156,9	78,6	219,2	284,8	298,5	299,5	920,7	269,9	11,2	*			-
18 (30-7-69)	84	11350	223,4	12,5	284,5	298,0	298,0	299,2	751,6	220,0	17,0	*			-
12 (30-7-69)	82,5	11320	225,4	16,0	279,7	292,0	296,7	298,2	790,0	231,6	16,6	*			-
4 (30-7-69)	82	10920	222,0	25,3	270,0	291,3	296,7	298,0	820,8	240,6	14,6	*			-

Burnout experiments data on channel B   TABLE VII

Nominal pressure: 100 ata

Run	Pressure ata	Flow l/h	Mass Flow rate gr/cm² sec.	Inlet °C Subcooling	Inlet °C Temperature	Exit temperature °C			Power Kw	Average heat flux watt/cm²	Exit quality %	Burnout rods position in the lattice			Pressure drop gr/cm²
						a	b	c				central	side	corner	
31 (15-2-68)	101,0	2460	49,5	35,3	274,9	307,5	308,9	–	450,2	131,9	50,4	*		*	94
43 (15-2-68)	96,0	2350	48,9	46,7	259,8	303,3	303,8	–	474,1	139,0	49,5	*		*	99
38 (5-3-68)	101,0	2360	49,2	51,4	258,9	–	–	–	475,5	139,4	48,4	*	*	*	110
64 (5-3-68)	98,5	2380	49,6	50,1	258,4	–	–	–	472,3	138,4	47,4	*	*	*	108
57 (15-2-68)	99,0	2350	49,6	56,2	252,6	304,7	305,7	–	489,9	143,6	47,9	*			99
49 (5-3-68)	103,5	2360	49,8	59,5	252,5	–	–	–	479,9	140,6	45,6	*			106
85 (15-2-68)	103,0	4290	81,0	12,4	299,2	307,0	307,0	–	506,2	148,3	39,5		*	*	175
95 (15-2-68)	105,0	4900	93,2	16,4	296,7	307,0	307,0	–	506,8	148,5	32,2		*	*	158
74 (1-3-68)	99,5	4780	92,6	18,9	290,2	304,0	–	–	542,0	158,8	33,5	*	*	*	120
77 (15-2-68)	105,0	4660	90,9	24,9	288,2	309,1	309,1	–	537,0	157,4	32,1	*			155
65 (15-2-68)	104,0	4660	92,2	29,9	282,5	308,7	308,7	–	542,9	159,1	29,8	*			116
20 (15-2-68)	106,0	4580	94,3	48,4	265,4	311,2	310,5	–	585,9	171,7	25,1	*			148

- 24 -

Burnout experiments data on channel B

TABLE VIII

Nominal pressure: 115 ata

Run	Pressure ata	Flow 1/h	Mass Flow rate gr/cm^{2}sec.	Inlet °C Subcooling	Inlet °C temperature	Exit temperature °C			Power Kw	Average heat flux watt/cm2	Exit quality %	Burnout rods position in the lattice			Pressure drop gr/cm2
						a	b	c				Central	Side	Corner	
62 (14-2-68)	116,0	2670	50,2	19,1	301,5	315,6	317,7	-	379,5	111,2	48,7	*	*	*	88
29 (5-3-68)	112,5	2640	50,2	20,5	297,7	-	-	-	392,9	115,1	49,4	*	*	*	97
25 (14-2-68)	115,5	2480	50,1	45,7	274,5	315,5	318,0	-	420,4	136,9	43,4	*			90
14 (5-3-68)	111,0	2520	51,0	43,7	273;5	-	-	-	434,2	127,3	44,6	*			97
9 (14-2-68)	114,0	2380	51,3	77,8	241,5	314,7	316,0	-	475,6	139,4	37,4	*			96
85 (14-2-68)	118,5	4920	92,7	21,0	301,2	319,0	319,0	-	465,8	136,5	28,6	*			-
51 (14-2-68)	114,5	4670	93,9	42,7	276,8	314,5	314,5	-	538,6	157,8	24,3	*			-

Burnout experiments data on channel B

TABLE IX

Nominal pressure: 132 ata

Run	Pressure ata	Flow 1/h	Mass Flow rate gr/cm² sec.	Inlet ° C Subcooling	Inlet °C Temperature	Exit temperature °C			Power Kw.	Average heat flux watt/ cm²	Exit quality %	Burnout Rods Position in the lattice			Pressure drop gr/cm²
						a	b	c				Central	Side	Corner	
86 (6-2-68)	132,0	2340	44,0	30,3	303,2	326,2	329,0	-	357,6	104,8	52,8	*			88
15 (20-5-69)	136,0	2641	49,7	31,3	301,5	314,8	332,0	333,2	341,5	100,1	39,9	*			-
19 (20-5-69)	133,5	2640	49,7	30,1	301,2	313,2	330,6	330,7	343,5	100,7	40,3	*			-
65 (1-3-68)	133,5	2600	49,9	34,9	296,5	-	-	-	357,2	104,7	41,2	*			89
115(19-1-68)	136,0	2610	51,2	44,1	288,7	-	328,7	-	363,0	106,4	36,5	*			-
63 (6-2-68)	130,5	2460	48,7	45,0	284,6	-	328,7	-	388,8	113,9	42,9	*			89
6 (20-5-69)	135,5	2526	49,7	47,8	284,6	315,3	332,4	332,7	364,2	106,8	35,9	*			-
3 (13-5-69)	131,2	2518	49,8	47,5	282,5	312,2	329,3	329,3	372,5	109,2	36,8	*			-
30 (2-2-68)	133,0	2700	54,9	57,8	273,2	-	-	-	397,7	116,6	31,2	*			68
69 (19-1-68)	131,0	2480	50,5	57,4	272,5	-	326,2	-	403,8	118,3	37,5	*			-
26 (20-5-69)	132,7	2414	50,0	70,1	260,7	311,8	330,3	330,7	408,5	119,8	32,7	*			-
8 (13-5-69)	133,1	2391	49,5	70,6	260,5	312,7	331,0	330,7	400,0	117,1	31,8	*			-
94 (19-1-68)	135,0	2360	50,0	79,2	253,0	-	328,0	-	431,6	126,5	33,8	*			-
31 (20-5-69)	132,5	2312	49,4	87,8	243,0	311,7	330,3	330,7	444,8	130,3	32,2	*			-
16 (13-5-69)	132,0	2308	49,5	89,5	241,0	311,7	330,0	330,0	450,3	132,0	32,3	*			-
5 (21-5-69)	131,5	2240	49,4	107,8	222,0	310,5	329,5	330,0	481,5	141,0	29,9	*			-
25 (13-5-69)	132,4	2237	49,5	109,7	221,0	312,1	330,5	330,2	477,0	139,8	28,6	*			-
14 (21-5-69)	136,0	2160	48,9	129,6	203,2	311,3	332,2	332,6	505,0	148,0	26,4	*			-
8 (21-5-69)	133,0	2160	48,9	128,1	203,0	310,6	330,6	330,9	503,5	147,5	26,7	*			-
32 (21-5-69)	134,0	4912	90,5	23,1	308,5	310,2	331,6	331,7	403,0	118,2	23,4	*			-
94 (6-2-68)	135,5	5000	93,6	27,5	305,0	-	328,4	-	417,6	122,4	22,2	*			124
25 (21-5-69)	132,5	4888	92,6	31,3	299,5	306,6	330,3	330,7	430,2	126,9	21,0	*			-
43 (19-1-68)	138,0	4960	95,2	37,2	296,7	-	-	-	425,8	124,8	17,5	*			-
32 (1-3-68)	132,0	4700	92,5	43,4	287,1	-	-	-	472,3	138,4	19,8	*			123
20 (21-5-69)	136,0	4670	92,8	52,3	280,5	297,2	332,1	332,6	463,0	135,7	14,2	*			-
75 (19-1-68)	134,0	4460	89,9	60,4	277,2	-	-	-	472,3	138,4	16,0	*			-

Run	Pressure ata	Flow l/h	Mass Flow rate gr/cm²sec.	Inlet °C Subcooling	Inlet °C Temperature	Exit temperature °C			Power Kw.	Average heat flux watt/cm²	Exit quality %	Burnout Rods Position in the lattice			Pressure drop gr/cm²
						a	b	c				Central	Side	Corner	
28 (22-1-68)	138,0	4240	86,6	62,5	271,5	-	-	-	504,2	147,8	17,3	*			-
18 (1-3-68)	134,5	4430	90,6	61,4	270,6	-	-	-	499,7	146,5	15,1	*			-
25 (22-1-68)	135,0	4470	92,4	66,5	265,7	-	-	-	500,0	146,5	12,0	*			-
42 (21-5-69)	133,5	4445	92,1	70,7	260,5	285,6	331,0	331,8	507,0	148,5	10,3	*			-
34 (6-2-68)	138,5	4200	87,8	73,8	260,4	-	330,2	-	497,3	145,7	10,8	*			-
50 (21-5-69)	133,0	4441	92,1	71,5	259,6	285,3	330,9	331,7	510,5	149,6	10,4	*			-
32 (6-2-68)	131,0	4270	90,0	74,8	255,1	-	326,0	-	516,5	151,4	11,3	*			-
57 (21-5-69)	133,2	4297	91,9	89,0	242,2	268,7	328,7	331,2	562,0	164,7	7,8	*			-
6 (22-5-69)	134,5	4228	90,8	92,2	239,7	271,6	330,6	331,8	570,0	167,0	7,7	*			-
18 (22-5-69)	133,7	4165	91,9	109,2	222,2	254,0	328,8	331,3	604,5	177,3	3,3	*			-
12 (22-5-69)	132,5	4147	92,0	112,3	218,5	254,5	328,1	330,8	613,0	179,6	2,9	*			-
28 (22-5-69)	132,5	4057	91,8	126,8	204,0	238,8	325,2	330,0	633,5	185,7	-0,8	*			-
22 (22-5-69)	132,7	4048	92,0	129,9	201,0	238,2	324,9	330,4	632,2	185,4	-2,3	*			-
21 (29-5-69)	134,2	7210	132,4	22,1	309,7	320,5	331,3	331,8	454,0	133,0	15,4	*			-
17 (29-5-69)	133,7	7000	131,8	30,0	301,5	318,2	331,8	332,3	491,0	144,4	14,0	*			-
13 (29-5-69)	133,9	7050	133,3	31,3	300,2	317,7	331,0	331,6	487,0	142,7	12,7	*			-
9 (29-5-69)	132,7	6750	133,8	49,4	281,5	312,0	330,0	330,7	555,5	162,8	8,6	*			-
5 (29-5-69)	135,2	6800	135,7	53,8	278,5	308,9	331,0	331,6	560,0	164,1	6,2	*			-
27 (29-5-69)	132,0	6560	133,1	59,5	271,0	305,0	330,0	330,5	580,0	170,0	5,8	*			-
39 (29-5-69)	131,7	6120	129,2	80,3	250,0	291,5	328,3	329,2	630,0	184,7	1,2	*			-
34 (29-5-69)	133,5	6280	132,7	82,0	249,4	291,2	329,2	330,1	632,2	185,3	-0,5	*			-
8 (30-5-69)	131,0	6120	132,7	96,1	233,7	290,5	327,6	329,2	675,0	197,8	-3,5	*			-
157(6-2-68)	131,0	8780	158,9	15,8	314,1	325,0	325,7	-	491,9	144,2	16,6	*			198
115 (6-2-68)	133,5	8480	156,9	23,0	308,4	326,7	327,5	-	486,5	142,6	12,9	*			194
23 (11-6-69)	133,0	7830	145,0	24,1	307,0	326,7	331,1	331,2	495,8	145,3	14,3	*			-
16 (11-6-69)	124,0	7860	148,7	31,6	300,0	325,2	331,6	331,8	522,0	153,0	11,4	*			-
56 (1-3-68)	131,0	8100	157,5	38,4	291,5	320,7	-	-	549,5	161,1	8,7	*			188
52 (6-2-68)	135,5	8000	158,5	47,9	284,6	322,9	325,2	-	582,5	170,7	5,6	*			182

Run	Pressure ata	Flow 1/h	Mass Flow rate gr/cm^{2}sec.	Inlet °C Subcooling	Inlet °C Temperature	Exit temperature °C			Power Kw.	Average heat flux watt/cm^2	Exit quality %	Burnout Rods Position in the lattice			Pressure drop$_2$ gr/cm^2
						a	b	c				Central	Side	Corner	
92 (19-1-68)	133,0	7980	158,3	47,1	284,0	323,0	-	-	560,4	164,2	5,0	*			174
19 (2-2-68)	131,0	7960	158,1	46,6	283,2	317,7	-	-	585,1	171,5	6,6	*			182
7 (11-6-69)	133,7	7470	148,1	50,0	281,5	318,2	331,5	331,6	588,0	172,3	6,8	*			-
11 (12-6-69)	136,0	7540	153,1	62,3	270,5	316,5	331,7	331,9	625,6	183,4	2,0	*			-
9 (2-2-68)	133,5	7550	154,8	61,8	269,6	313,7	-	-	601,3	176,2	1,3	*			165
18 (12-6-69)	132,3	7420	153,7	70,1	260,5	312,2	330,0	330,2	673,7	197,5	1,4	*			-
25 (12-6-69)	130,5	7170	150,8	76,3	252,2	308,7	329,2	329,3	702,0	205,8	0,7	*			-
32 (12-6-69)	131,7	6940	148,5	88,0	242,2	304,7	329,1	328,7	731,3	214,2	-1,5	*			-
54 (12-6-69)	132,7	6715	146,6	101,4	229,5	294,0	328,8	328,7	766,8	224,7	-4,6	*	*		-
41 (12-6-69)	131,7	6715	148,2	108,0	222,2	290,7	328,0	327,2	795,2	233,1	-6,0	*	*		-
47 (12-6-69)	132,0	6695	148,4	111,2	219,2	284,7	327,3	327,2	802,7	235,3	-7,0		*		-
144 (6-2-68)	132,0	12230	225,4	21,1	309,4	326,2	326,7	-	577,0	169,1	9,3	*			289
27 (2 - 7-69)	131,7	12560	232,0	21,9	308,4	320,7	327,2	329,6	603,0	176,7	8,6	*			-
49 (2-2-68)	133,0	12000	226,4	28,8	302,2	326,7	-	-	610,8	179,0	6,6	*			258
33 (2-7-69)	131,9	12440	237,0	31,6	298,7	317,3	324,0	329,4	671,2	196,7	5,9	*			-
126(19-1-68)	136,5	11890	227,3	34,9	298,2	-	-	-	619,1	181,5	3,6	*			200
21 (2-7-69)	131,2	11840	230,0	39,5	290,5	314,2	327,2	329,5	721,4	211,4	4,8	*			-
41 (2-7-69)	134,3	11640	231,0	50,3	281,5	307,6	316,7	330,7	755,8	221,6	0,8	*			-
20 (2-7-69)	132,5	11280	230,0	61,9	268,9	302,7	319,2	329,9	835,6	244,8	- 1,2	*			-
16 (2-7-69)	132,4	10860	227,0	73,2	257,5	294,6	313,0	329,4	889,5	260,6	-3,6	*	*		-
46 (2-7-69)	131,4	10860	229,0	77,4	252,7	289,0	305,0	328,7	920,0	269,6	-4,5	*			-

Burnout experiments data on channel B

TABLE X

Nominal pressure: 144 ata

Run	Pressure ata	Flow 1/h	Mass Flow rate gr/cm^{2}sec.	Inlet °C Subcooling	Inlet °C Temperature	Exit temperature °C			Power Kw.	Average heat flux watt / cm^2	Exit quality %	Burnout rods position in the lattice			Pressure drop gr/cm^2
						a	b	c				Central	Side	Corner	
105(16-7-68)	147,5	2650	50,2	37,0	302,2	332,2	337,1	337,2	341,0	99,9	38,9	*	*		88
91(16-7-68)	145,0	2060	41,4	58,5	279,3	335,5	333,8	336,3	386,1	113,2	51	*			90
65(16-7-68)	146,0	2400	50,9	85,7	252,7	335,8	337,2	337,0	435,0	127,5	31	*	*		94
60(21-12-67)	143,0	4760	91,0	38,0	298,7	332,2	335,2	333,5	407,7	119,5	17,2	*			-
16(19-1-68)	144,0	4840	93,5	42,3	295,0	332,7	-	-	410,0	120,2	14,2	*			-
8(17-6-68)	145,5	4600	91,2	52,9	285,2	334,8	335,8	336,6	451,8	132,4	14	*	*		126
55(16-7-68)	145,0	4480	94,8	83,8	254,0	316,6	336,6	335,5	517,6	151,7	4	*	*		131
25(19-1-68)	140,0	8210	158,8	40,8	294,3	327,5	309,3	-	512,6	150,2	4,9	*			-
46(16-7-68)	144,5	7480	151,0	60,1	277,5	323,1	333,6	334,6	621,9	182,3	3,1	*	*		-
50(16-7-68)	145,5	7480	151,4	61,9	276,2	323,8	333,7	335,1	626,5	183,6	2,3	*	*		183
132(19-1-68)	142,0	12280	226,6	25,8	.310,4	329,1	-	-	578,7	169,6	6,6	*			263
16(16-7-68)	144,0	11800	221,4	32,3	305,0	331,2	336,2	336,7	634,4	185,9	5,8	*			291

Burnout experiments data on channel B

TABLE XI

Nominal Pressure: 158 ata

Run	Pressure ata	Flow l/h	Mass Flow rate gr/cm²sec.	Inlet °C Subcooling	Inlet °C Temperature	Exit temperature °C			Power Kw.	Average heat flux watt/cm²	Exit quality%	Burnout rods position in the lattice			Pressure drop gr/cm²
						a	b	c				central	side	corner	
23 (4-7-69)	157,0	8695	156,0	26,7	317,5	332,6	343,0	343,4	463,0	135,7	9,1	*			–
26 (4-7-69)	156,7	8405	155,0	35,1	309,0	329,5	341,5	343,4	491,3	144,0	5,9	*			–
21 (4-7-69)	159,2	8127	155,0	46,1	298,7	322,6	340,7	345,4	545,0	159,7	2,7	*			–
14 (4-7-69)	157,8	7931	155,0	50,3	289,0	316,3	336,2	344,0	565,0	165,7	– 0,8	*			–
9 (4-7-69)	157,0	7745	155,0	64,2	280,0	311,2	331,2	343,2	598,5	175,4	– 3	*			–
36 (4-7-69)	157,0	7395	153,0	81,7	262,5	300,6	324,0	342,6	674,5	197,7	– 6,8	*			–
43 (4-7-69)	157,5	7158	154,0	104,2	240,2	289,0	314,0	340,0	773,0	226,6	-12,1	*			–
37 (3-7-69)	159,0	17098	301,0	23,2	322,0	332,5	341,7	344,5	700,0	205,2	5	*			–
28 (3-7-69)	158,5	16727	297,0	25,0	320,0	331,4	341,0	344,9	709,4	207,9	4,4	*			–
34 (30-7-69)	158,0	16975	301,7	25,7	319,0	335,3	345,0	343,7	748,2	219,2	4,8	*			–
25 (30-7-69)	158,5	15905	288,7	32,0	313,0	332,8	345,1	344,2	783,8	229,8	3,2	*			–
23 (3-7-69)	159,0	16130	295,0	34,0	311,2	327,2	337,5	345,4	781,2	229,0	1,3	*			–
14 (3-7-69)	157,7	16562	309,0	39,6	305,0	321,8	334,0	343,6	851,5	249,6	– 0,7	*			–
38 (30-7-69)	154,0	15490	289,3	38,4	304,2	328,5	343,2	342,5	843,6	247,2	1,8	*			–
48 (3-7-69)	157,5	15615	294,0	48,2	302,2	319,8	334,4	343,6	842,6	246,9	– 1,1	*			–
56 (3-7-69)	157,5	15285	297,0	53,7	290,7	313,2	330,0	342,9	926,5	271,6	– 4,9	*			–
63 (3-7-69)	157,4	15059	295,0	56,8	287,6	311,5	328,7	342,5	950,3	278,6	– 5,5	*			–

TABLE XII

Interpretation Key of the symbols employed in the graphical representations of Fig. 6 through 25

○   Burn-out detected on the central rod only

▯   Burn-out detected on the lateral rod only

◸   Burn-out detected on the corner rod only

⌓   Burn-out detected on the central and lateral rods

◇   Burn-out detected on the central and corner rods

▢   Burn-out detected on the lateral and corner rods

△   Burn-out detected on the central, lateral and corner rods

Black symbols refer to channel   A

Open symbols refer to channel   B.
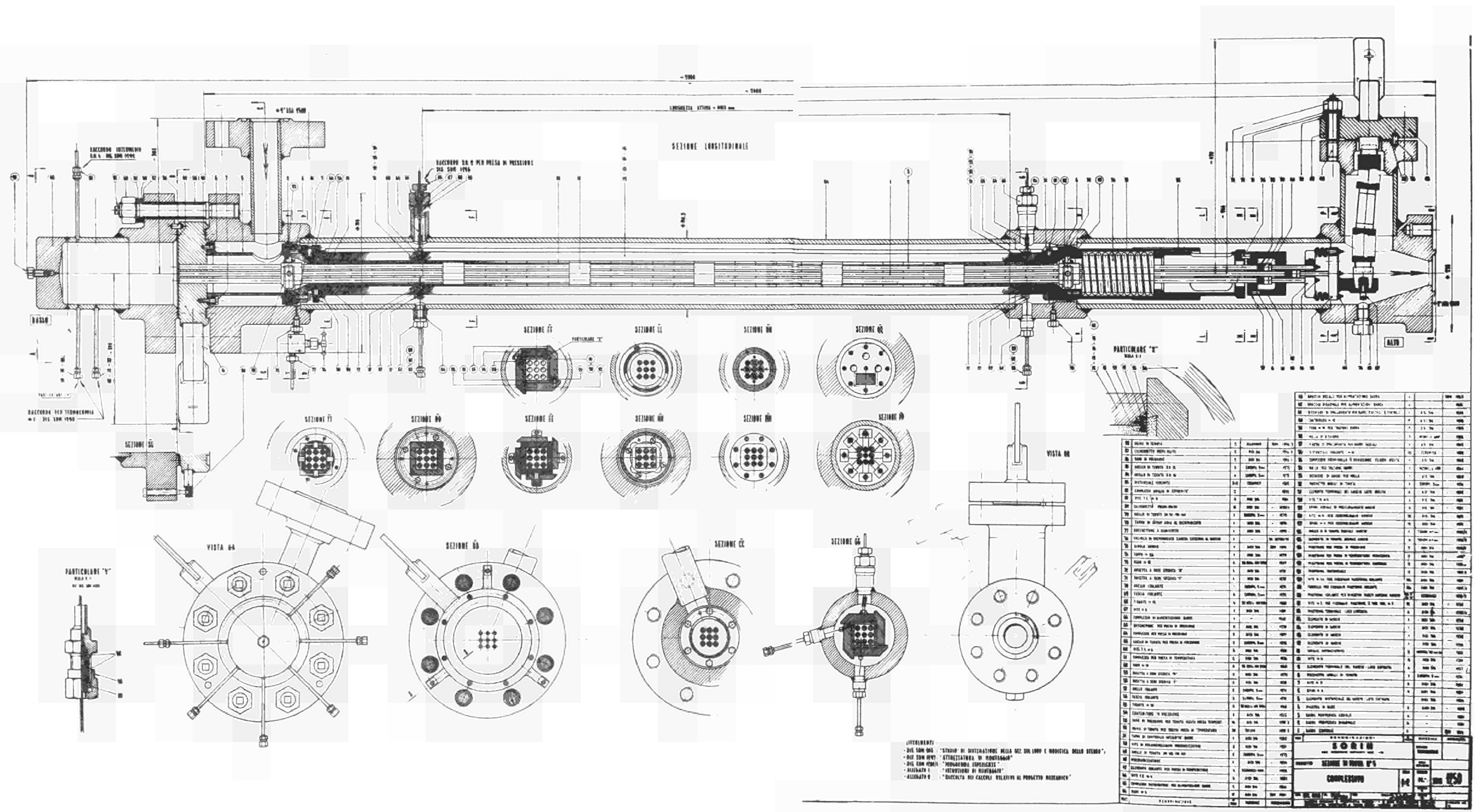
Fig. 1 : Test section assembly drawing
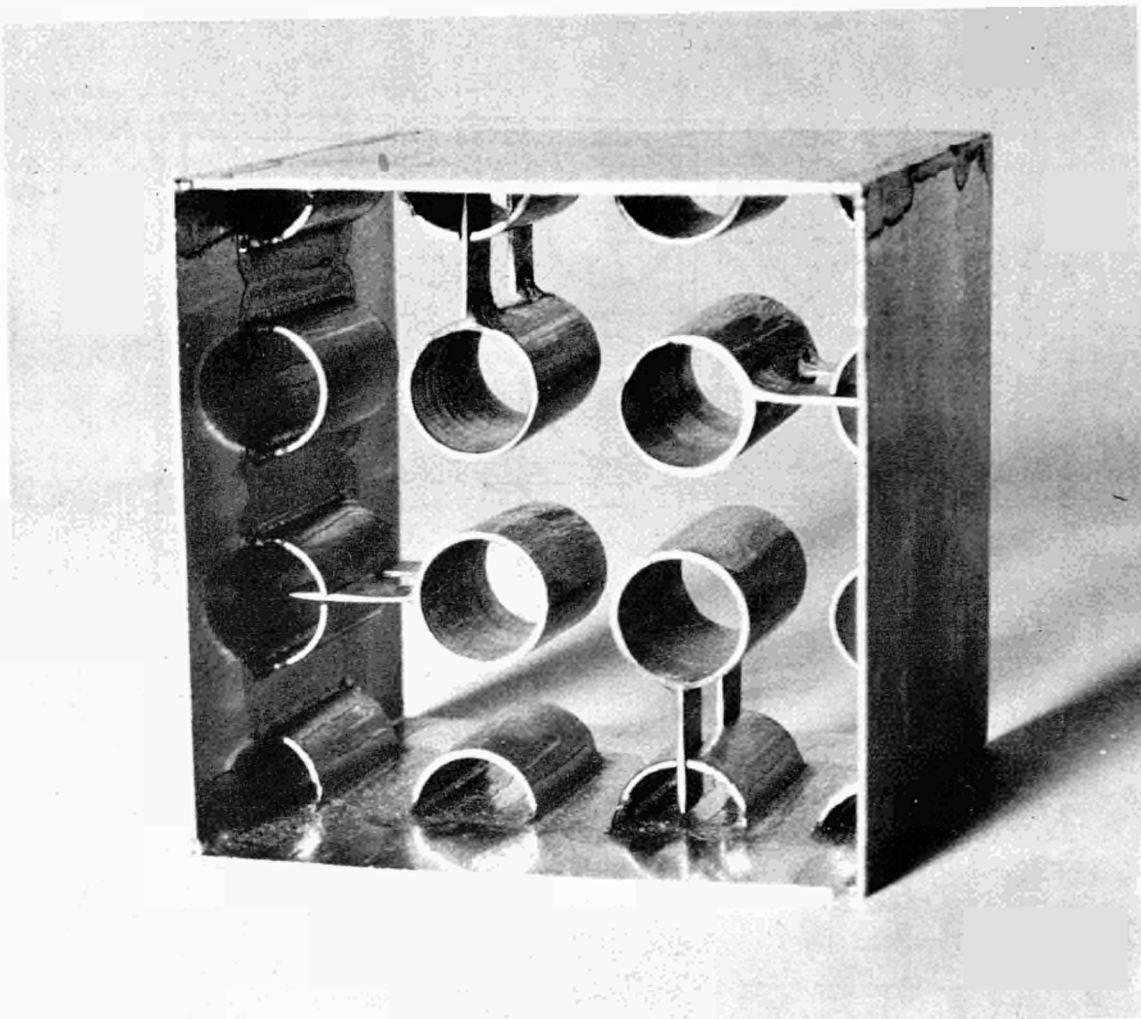
Fig. 2 - Close-up view of the grid.
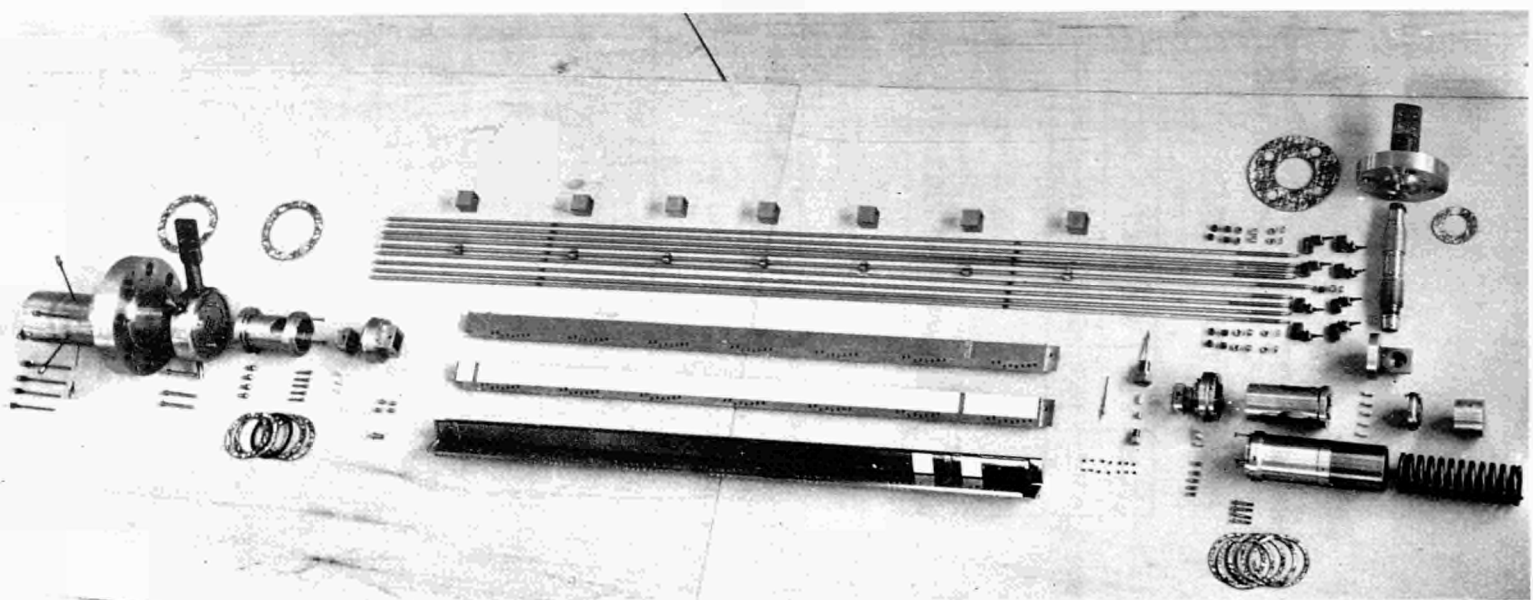
Fig. 3 - Exploded view of the test section
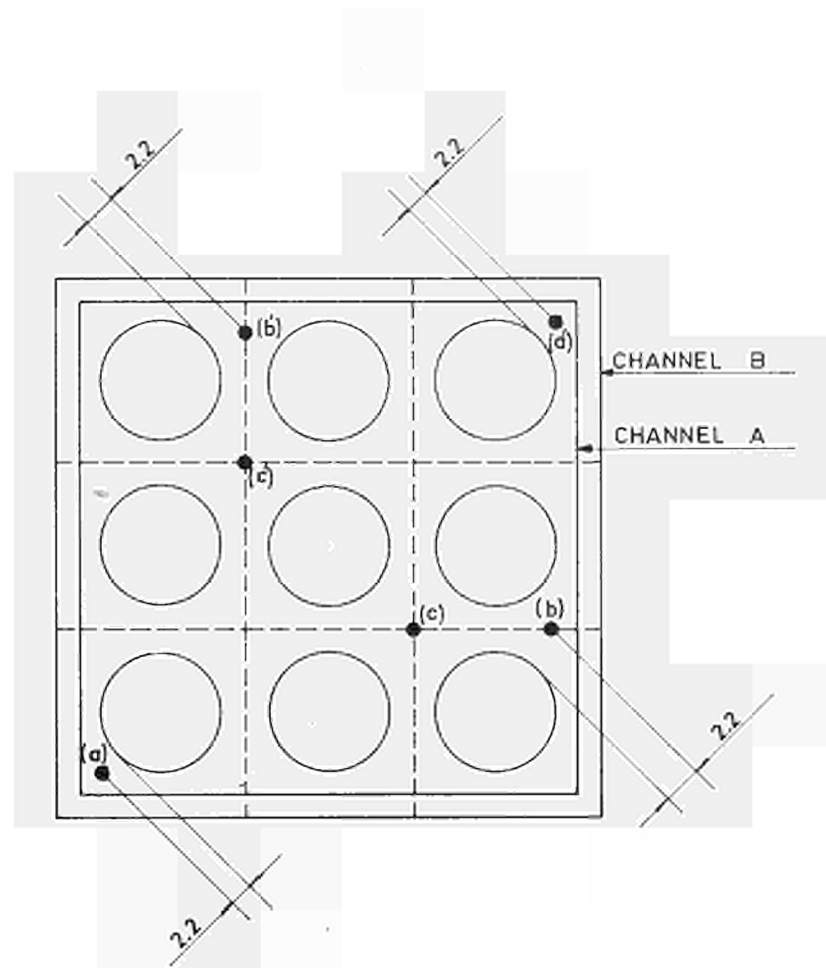
Fig. 4 – Schematic cross section of the channel showing location of the water exit temperature probes.
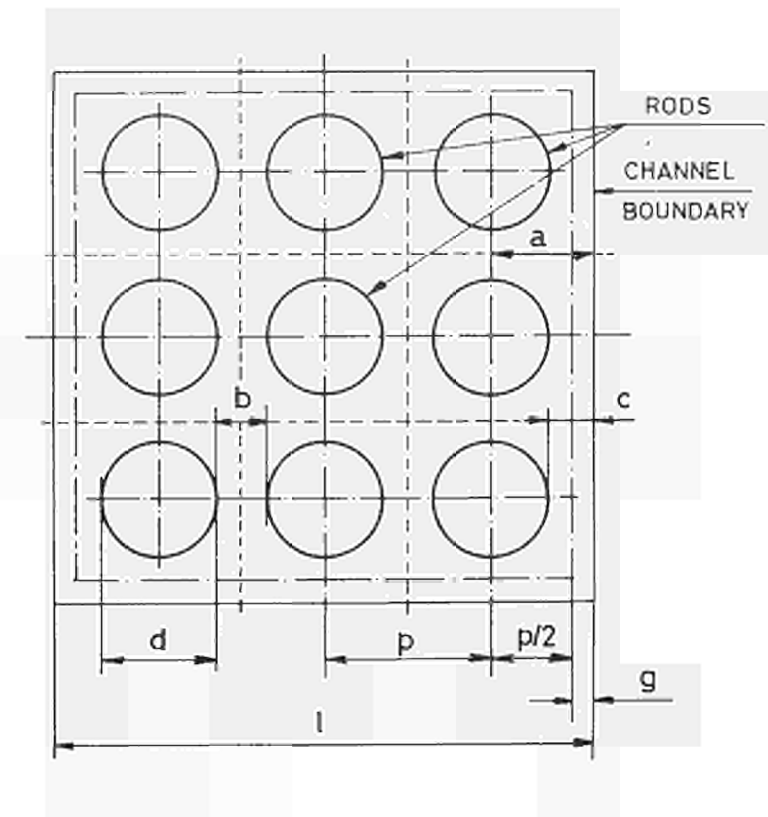
CHANNEL TYPE	DIMENSIONS (mm)						
	d	p	b	g	a	c	l
A	10,20	13,40	3,20	0,00	6,70	1,60	40,20
B	10,20	13,40	3,20	1,06	7,76	2,66	42,32

Fig. 5 – Schematic cross section of the tested channels A and B showing their most relevant dimensions.
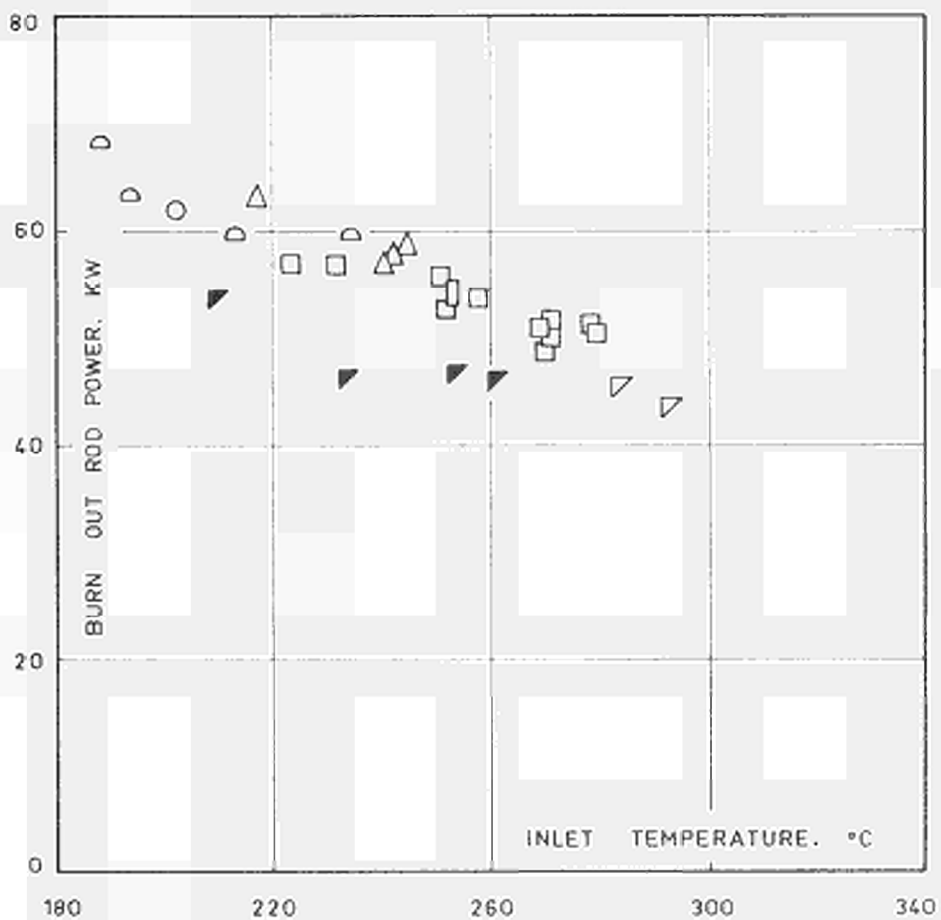
Fig. 6 – Burn-out experiments on channels A and B at 84 ata
nominal pressure and 50 gr/cm² sec nominal mass
flow rate.
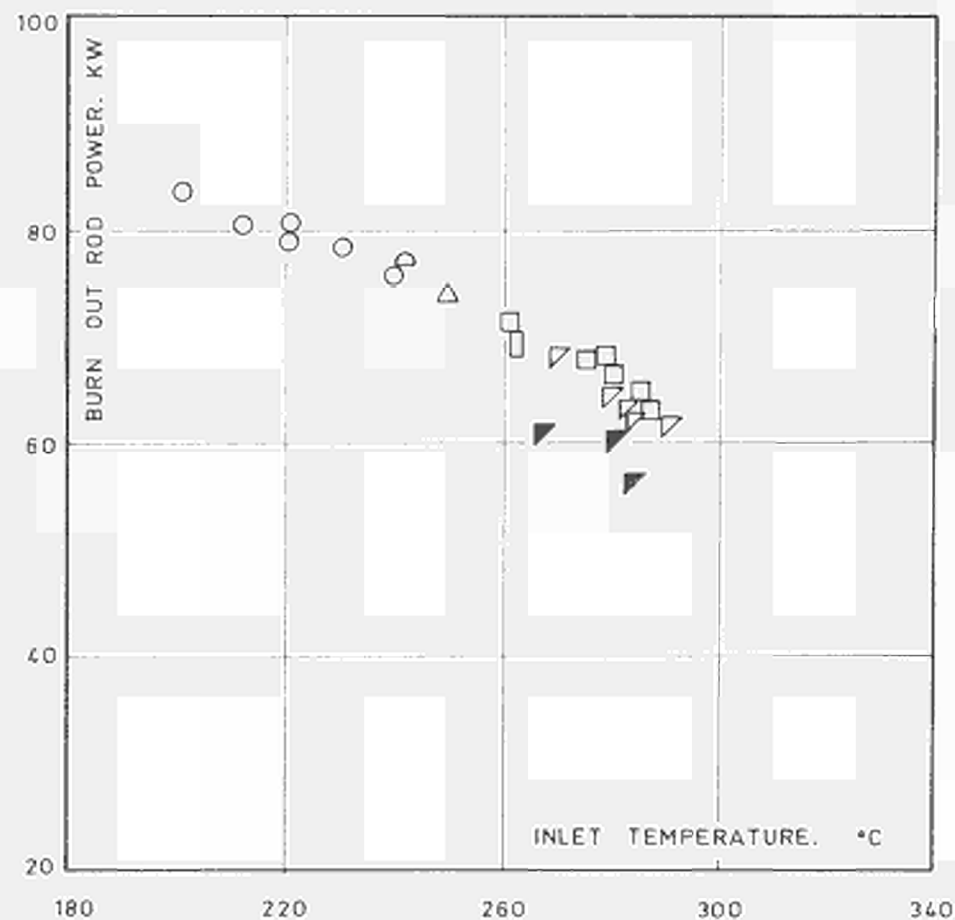
Fig. 7 – Burn-out experiments on channel A and B at 84 ata
nominal pressure and 93 gr/cm² sec nominal mass
flow rate.
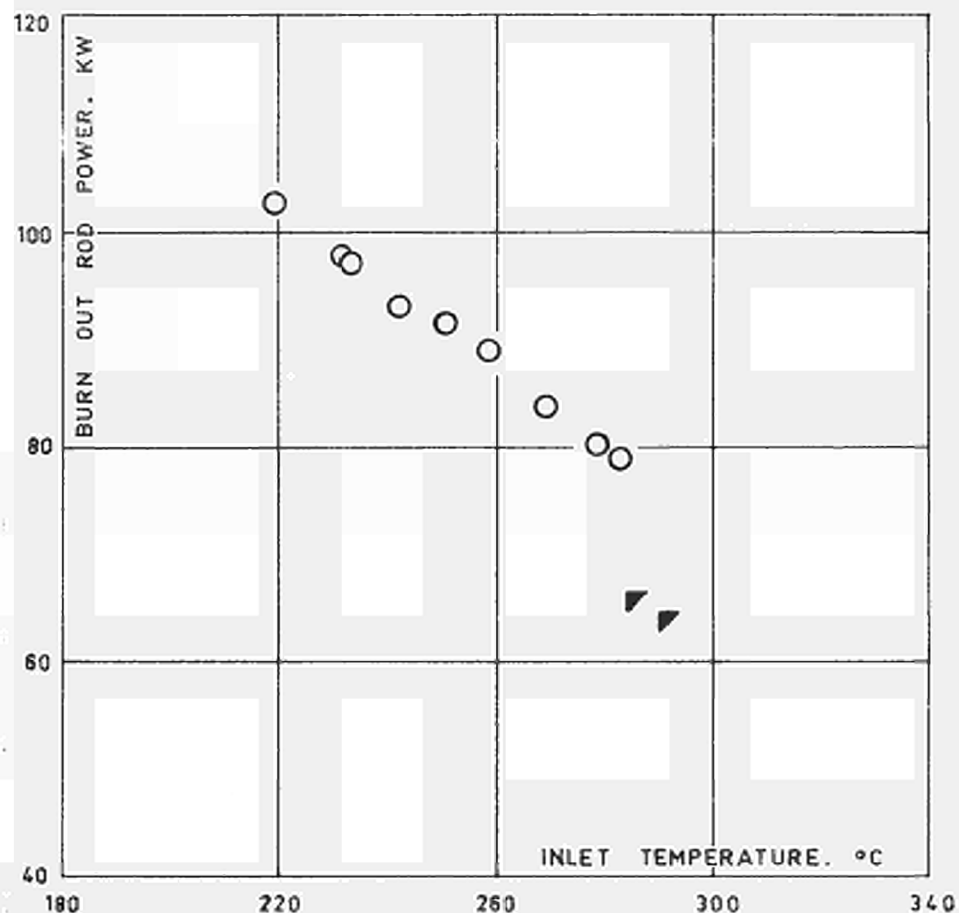
Fig. 8 – Burn-out experiments on channels A and B at 84 ata nominal pressure and 156 gr/cm² sec nominal mass flow rate.
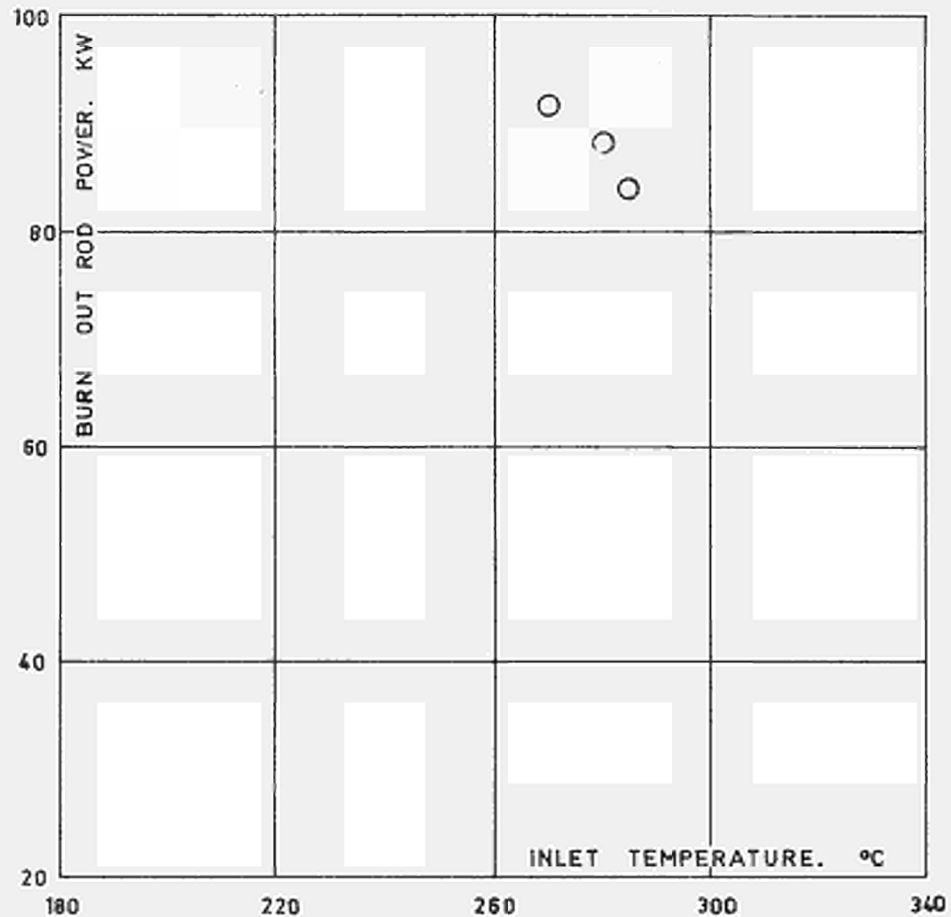
Fig. 9 – Burn-out experiments on channel B at 84 ata nominal pressure and 225 gr/cm² sec nominal mass flow rate.
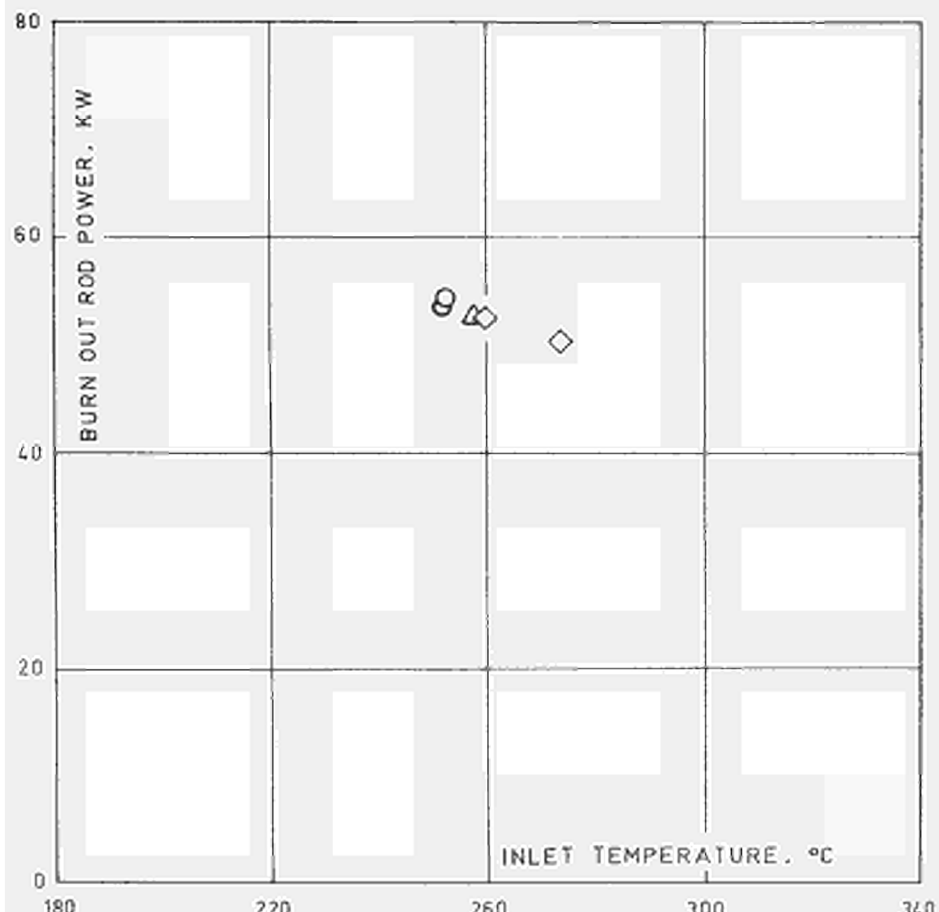
Fig. 10 – Burn-out experiments on channel B at 100 ata nominal pressure and 50 gr/cm² sec nominal mass flow rate.
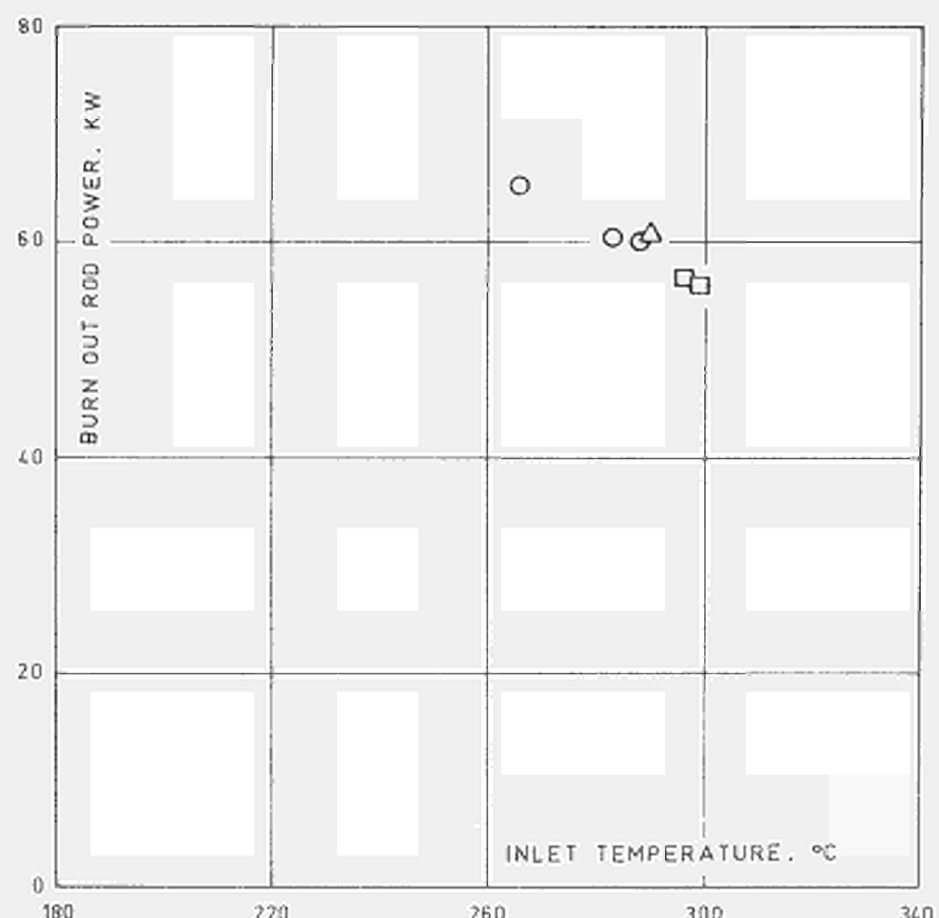
Fig. 11 – Burn-out experiments on channel B at 100 ata nominal pressure and 93 gr/cm² sec nominal mass flow rate.
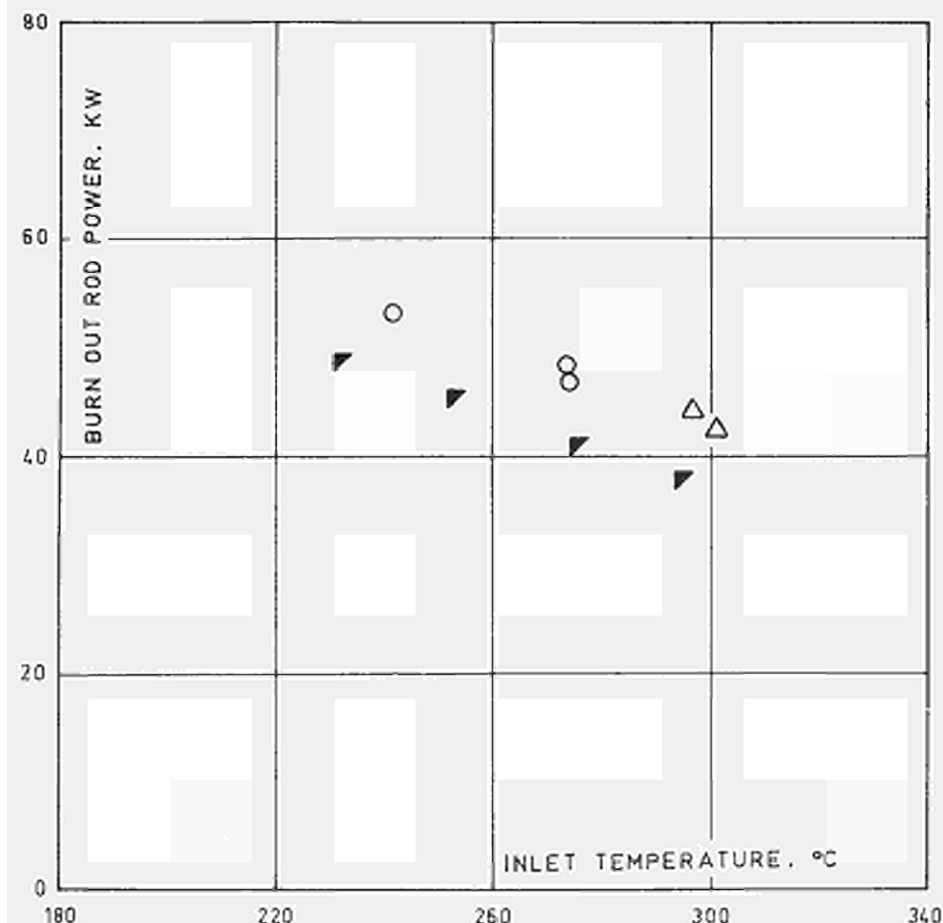
Fig. 12 – Burn-out experiments on channels A and B at 115 ata nominal pressure and 50 gr/cm² sec nominal mass flow rate.
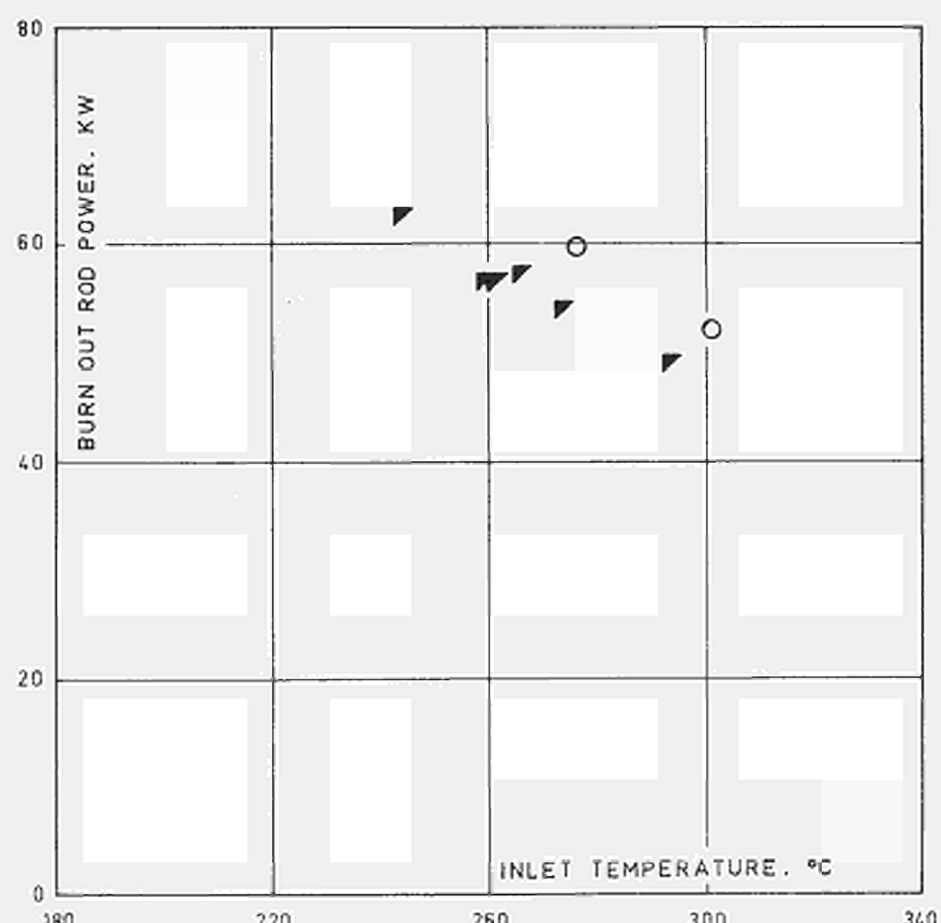
Fig. 13 – Burn-out experiments on channels A and B at 115 ata nominal pressure and 93 gr/cm² sec nominal mass flow rate.
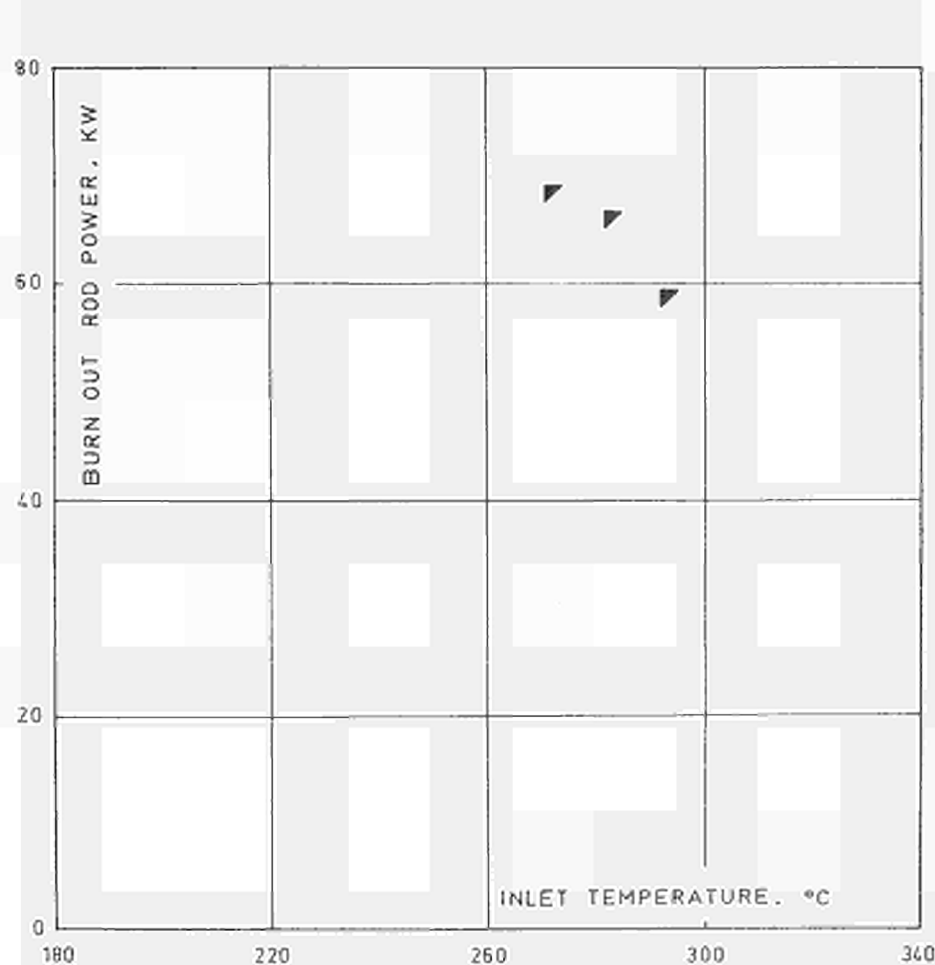
Fig. 14 - Burn-out experiments on channel A at 115 ata nominal pressure and 156 gr/cm² sec nominal mass flow rate.
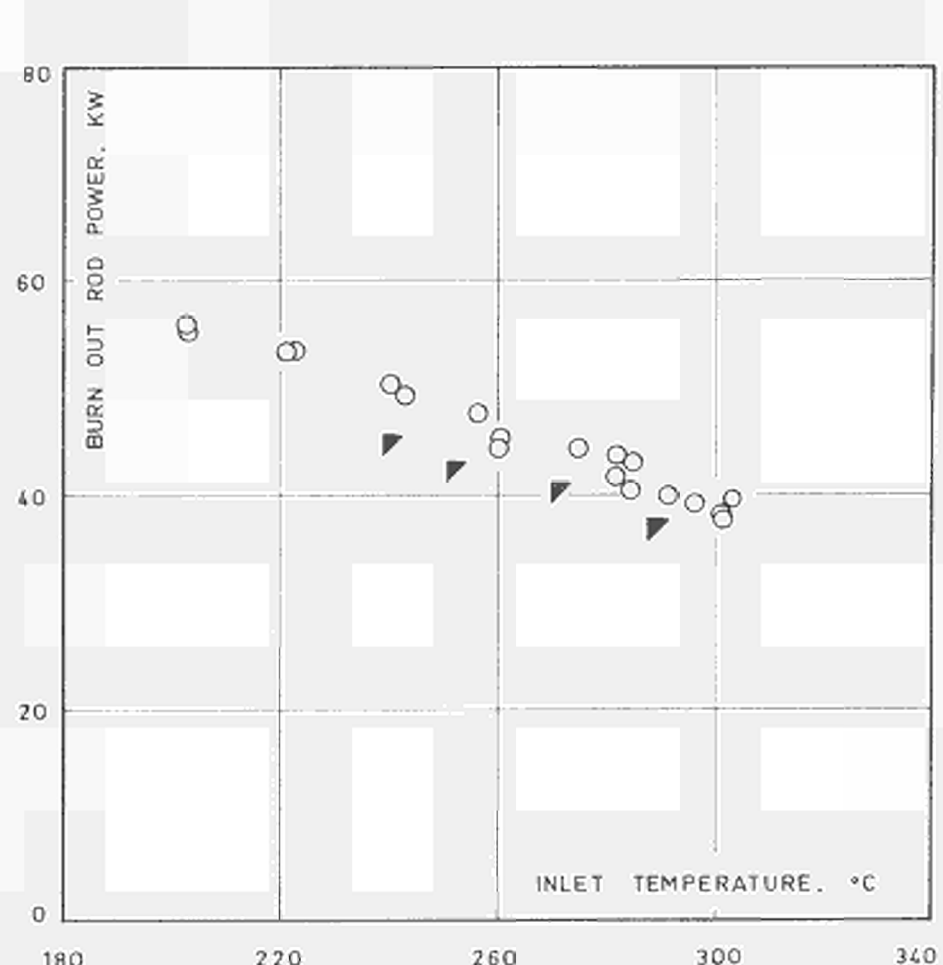

Fig. 15 - Burn-out experiments on channel A and B at 132 ata nominal pressure and 50 gr/cm² sec nominal mass flow rate.
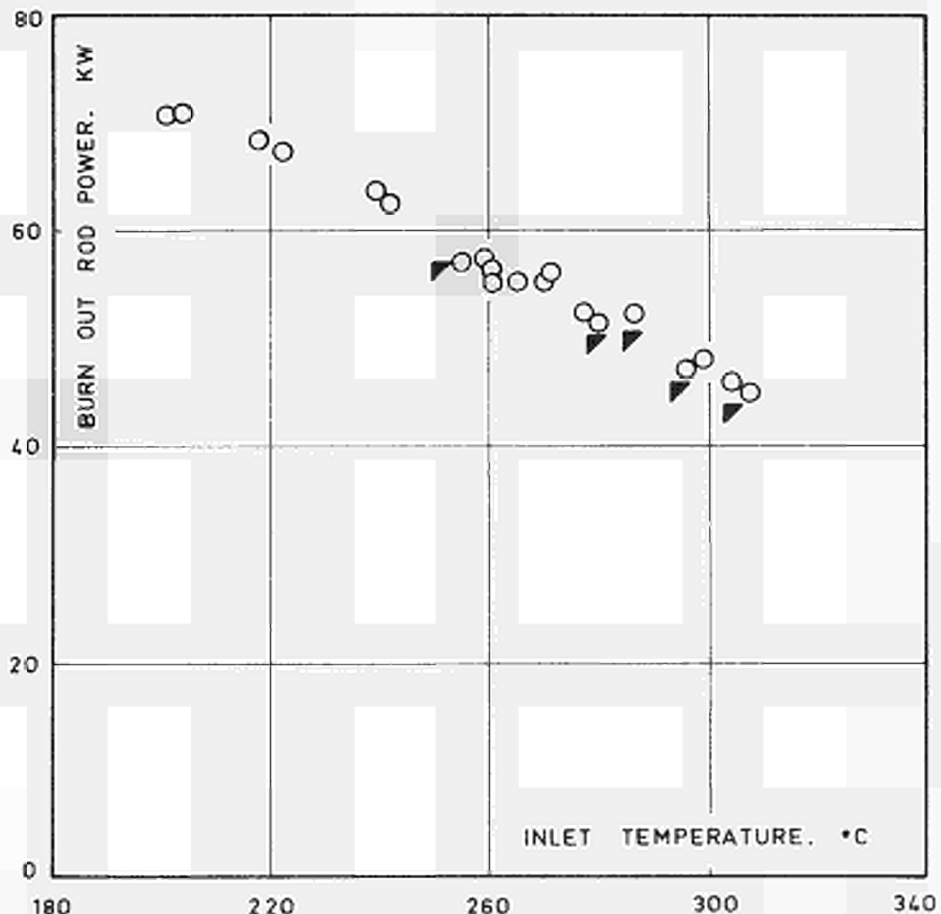
Fig. 16 - Burn-out experiments on channels A and B at
132 ata nominal pressure and 91 gr/cm² sec
nominal mass flow rate.
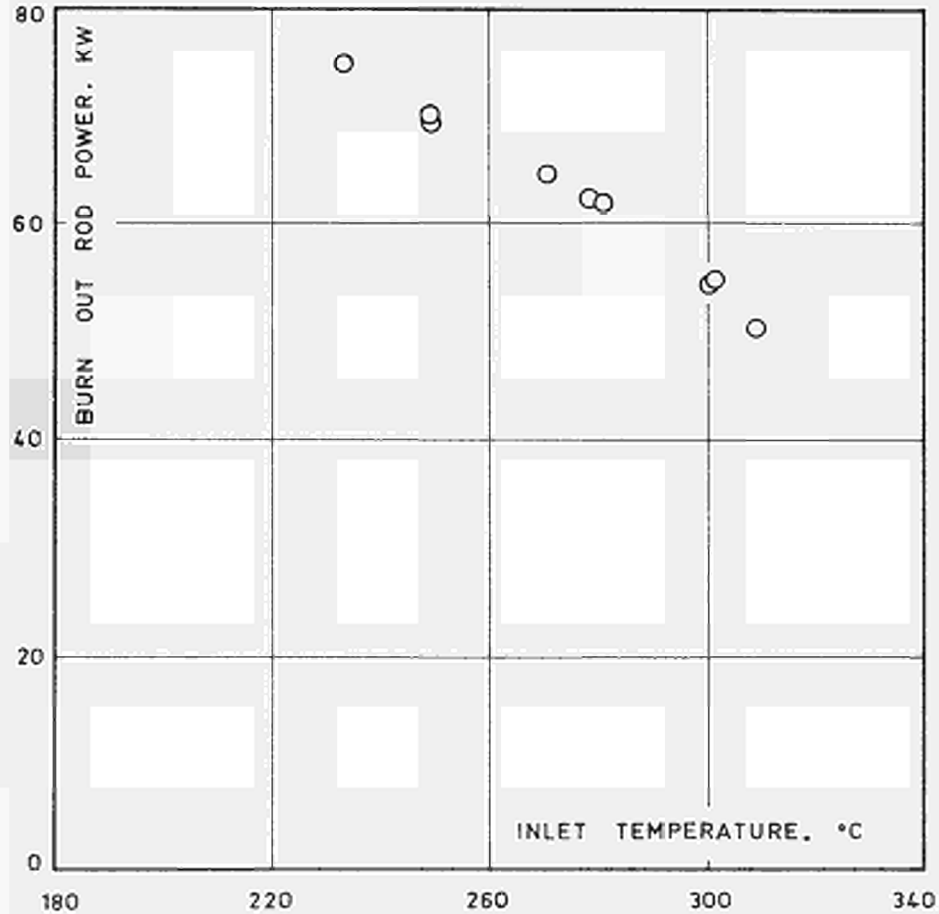
Fig. 17 - Burn-out experiments on channel B at 132 ata
nominal pressure and 133 gr/cm² sec nominal
mass flow rate.
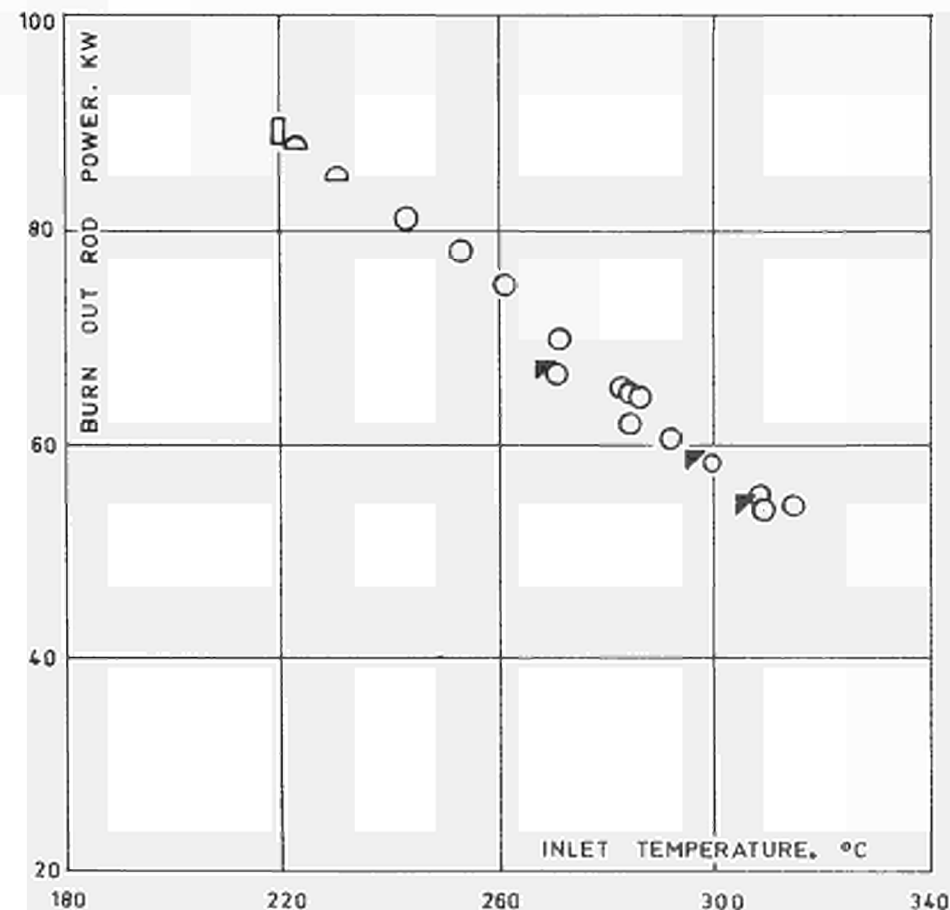
Fig. 18 – Burn-out experiments on channels A and B at 132 ata nominal pressure and 156 gr/cm² sec nominal mass flow rate.
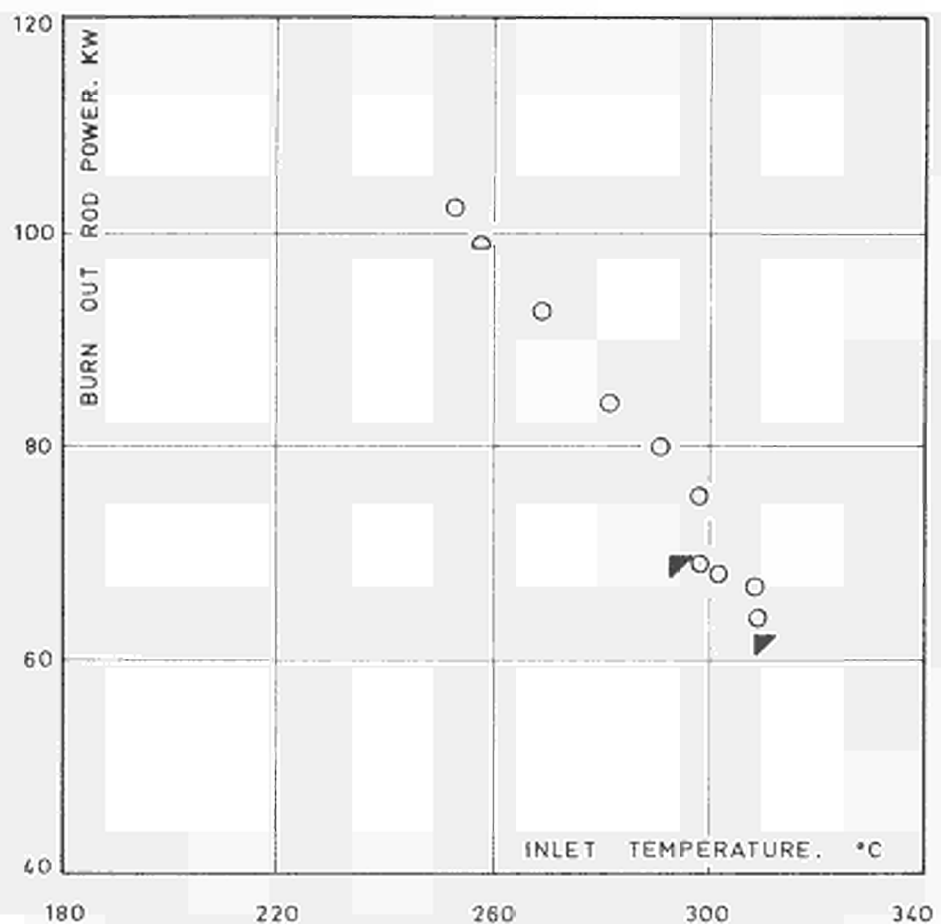
Fig. 19 – Burn-out experiments on channel A and B at 132 ata nominal pressure and 225 gr/cm² sec nominal mass flow rate.
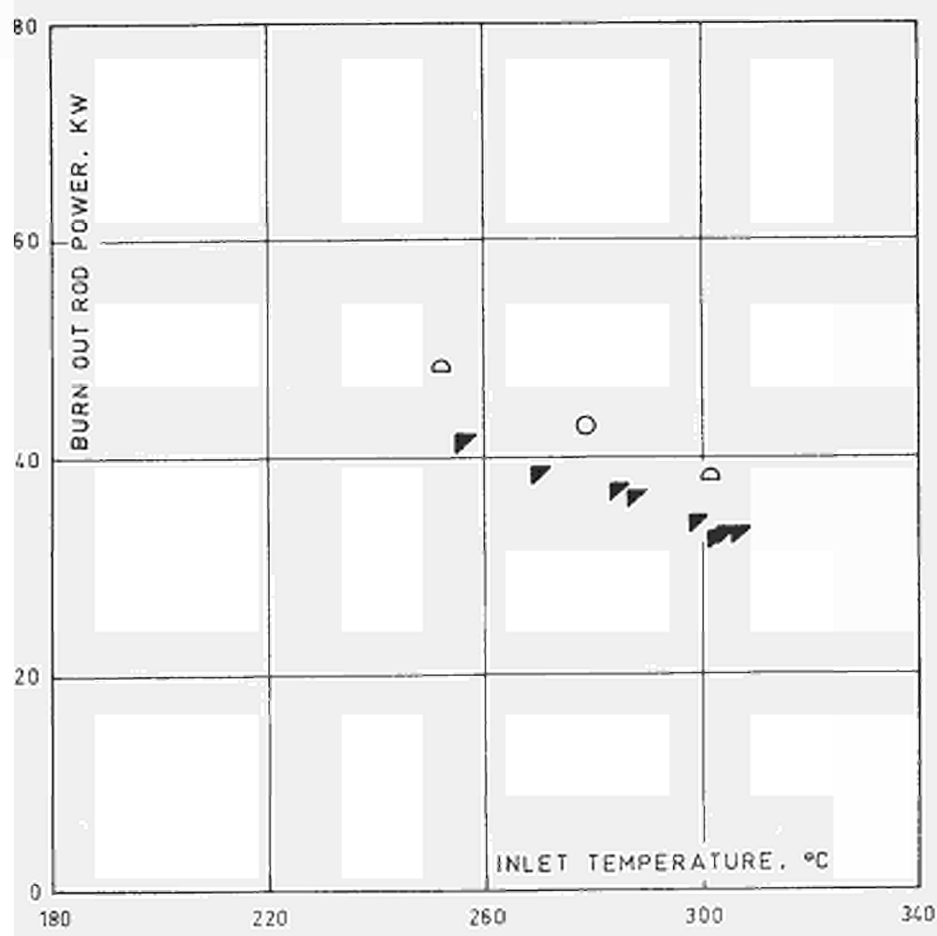
Fig. 20 - Burn-out experiments on channels A and B at
144 ata nominal pressure and 50 gr/cm² sec
nominal mass flow rate.
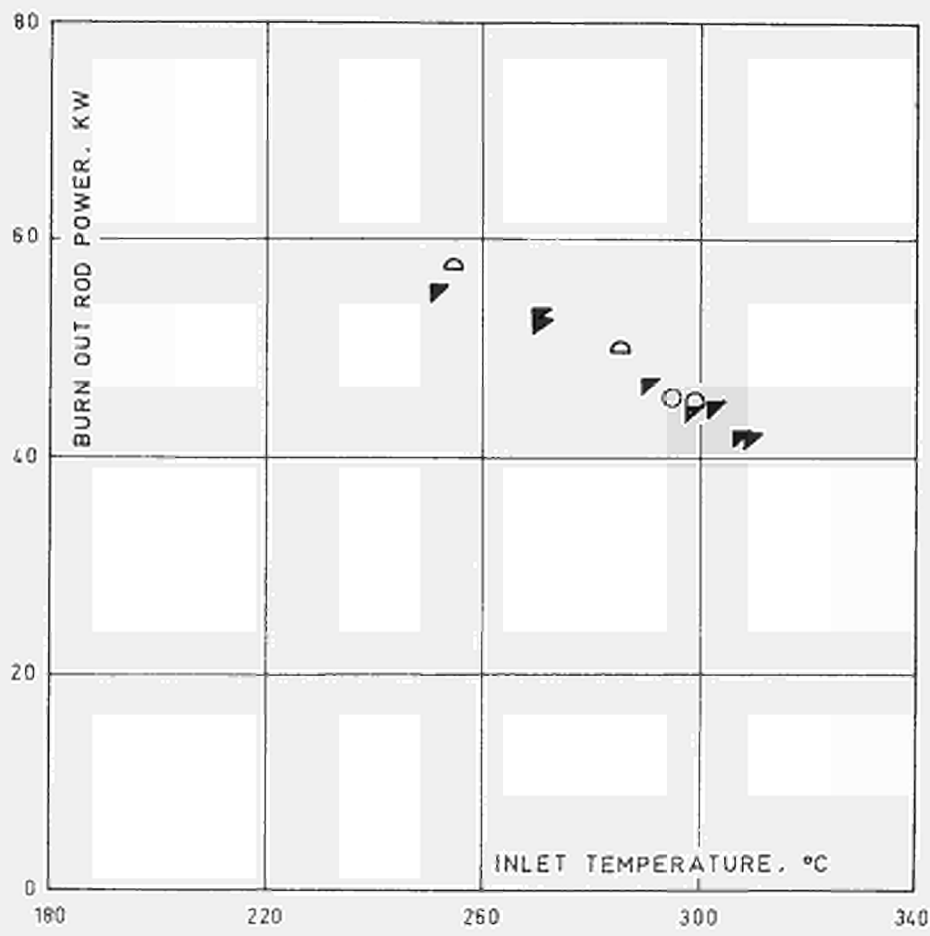
Fig. 21 - Burn-out experiments on channels A and B at
144 ata nominal pressure and 93 gr/cm² sec
nominal mass flow rate.
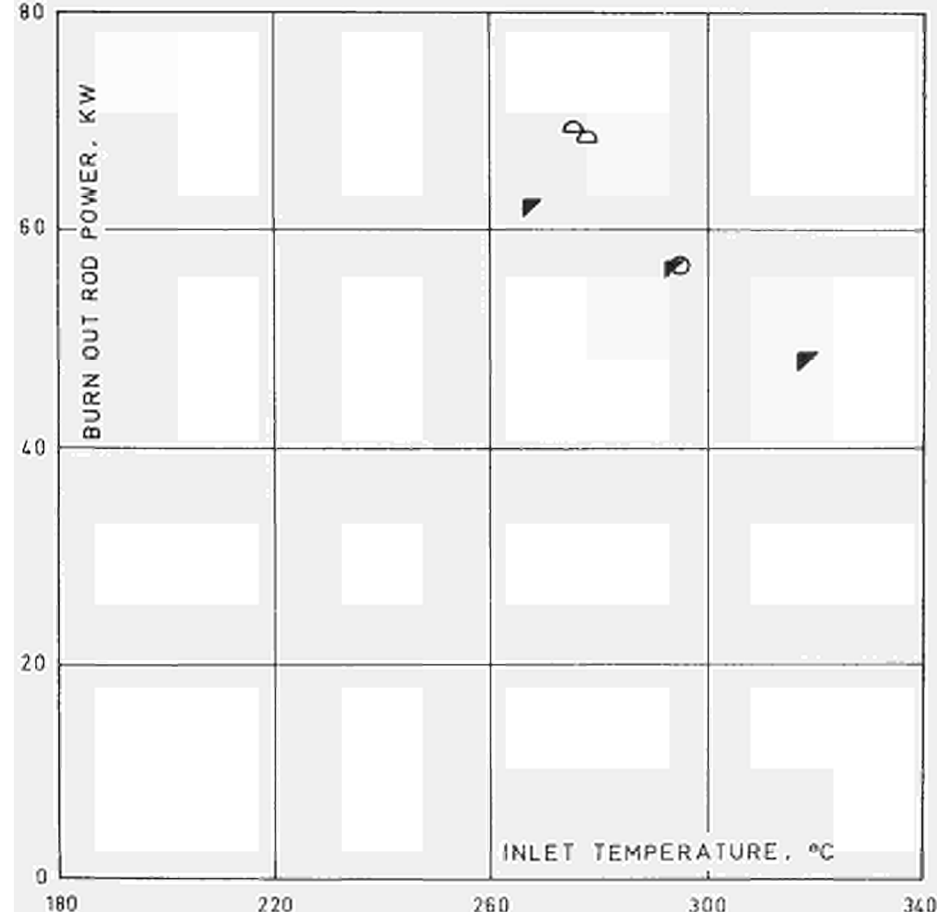
Fig. 22 - Burn-out experiments on channels A and B at
144 ata nominal pressure and 156 gr/cm² sec
nominal mass flow rate.
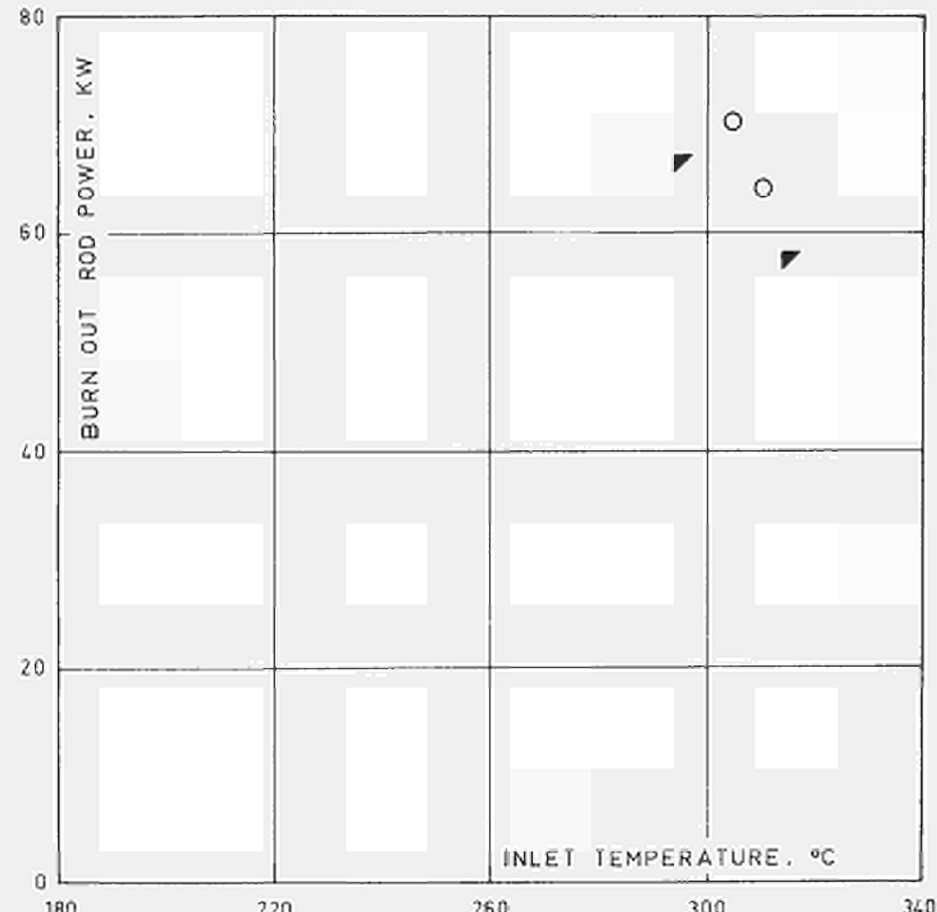
Fig. 23 - Burn-out experiments on channels A and B at
144 ata nominal pressure and 225 gr/cm² sec
nominal mass flow rate.
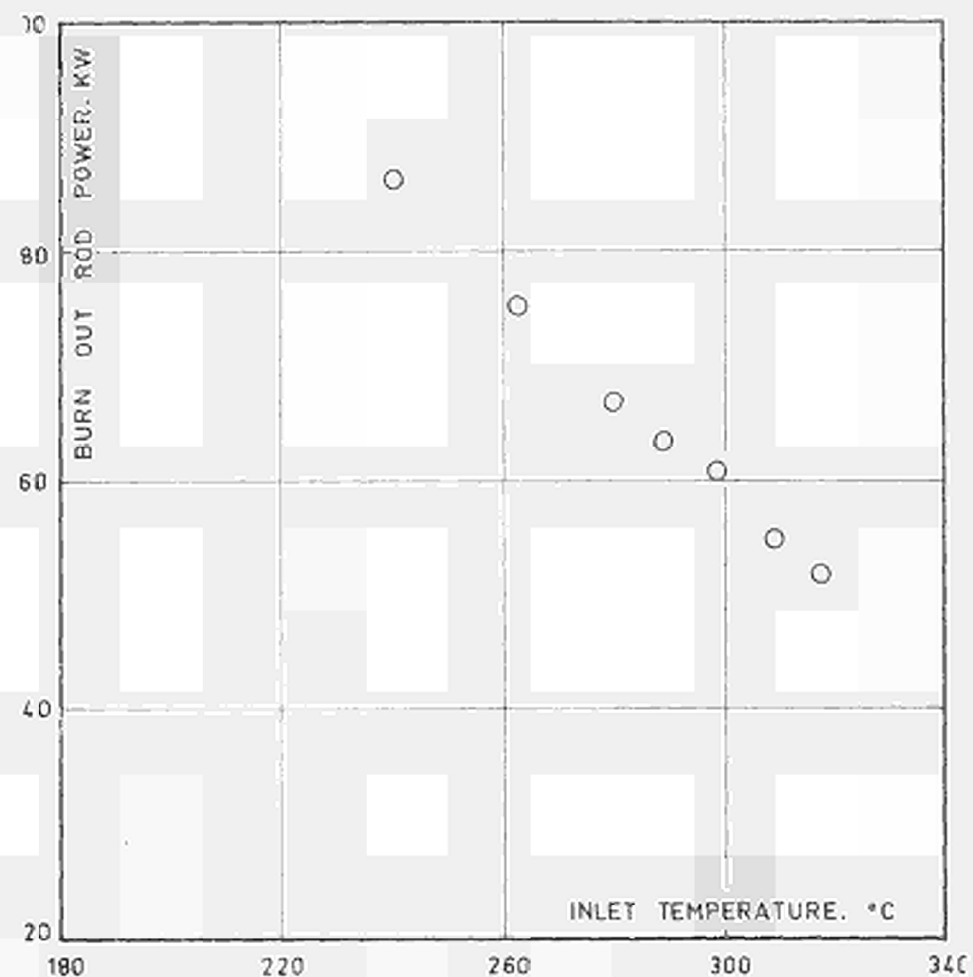
Fig. 24 – Burn-out experiments on channel B at 158 ata nominal pressure and 156 gr/cm² sec nominal mass flow rate.
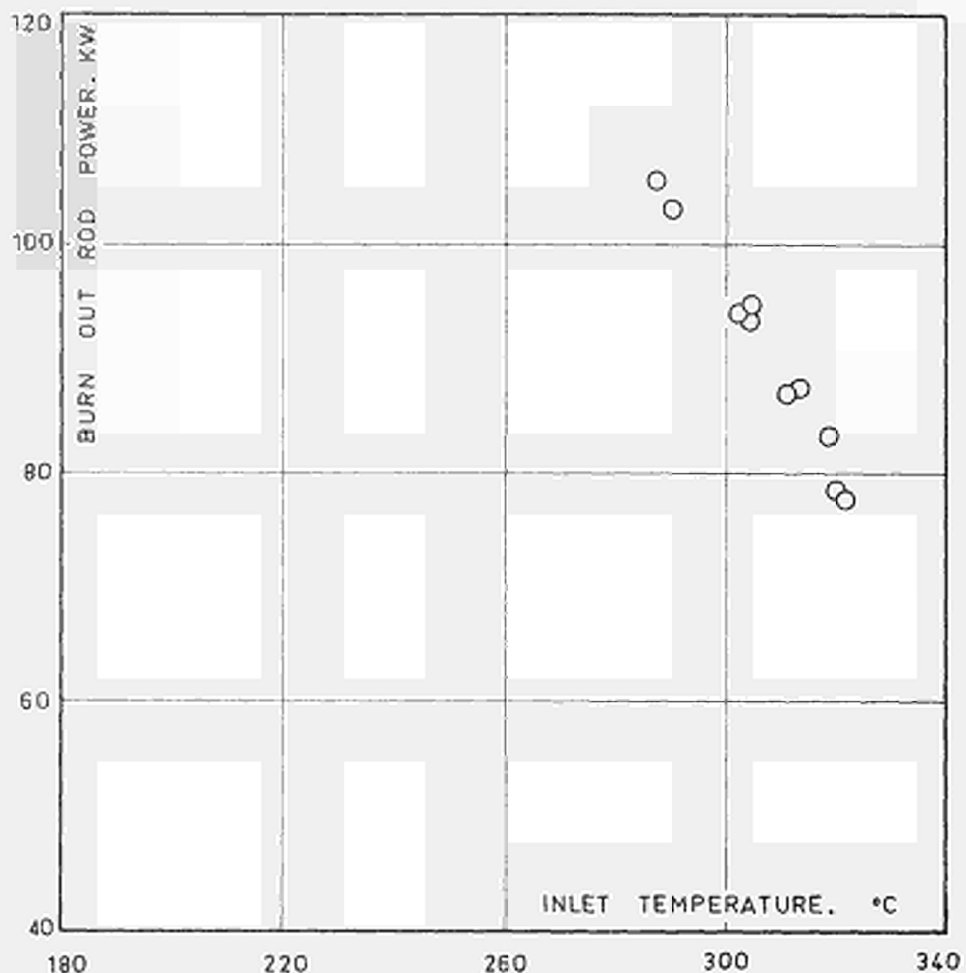
Fig. 25 – Burn-out experiments on channel B at 158 ata nominal pressure and 300 gr/cm² sec nominal mass flow rate.
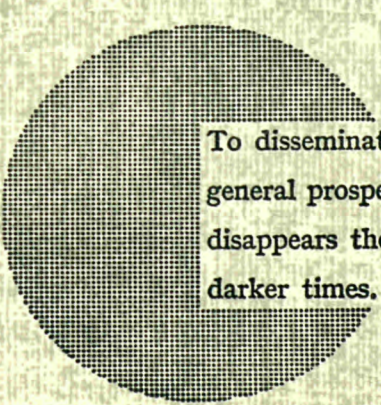
To disseminate knowledge is to disseminate prosperity — I mean general prosperity and not individual riches — and with prosperity disappears the greater part of the evil which is our heritage from darker times.

Alfred Nobel

SALES OFFICES

All reports published by the Commission of the European Communities are on sale at the offices listed below, at the prices given on the back of the front cover. When ordering, specify clearly the EUR number and the title of the report which are shown on the front cover.